THE VARIABILITY OF PRECIPITATION PATTERNS OVER THE CENTRAL AND WEST PACIFIC OCEAN

BY

Kevin James Edward Walsh

SUBMITTED TO THE DEPARTMENT OF METEOROLOGY AND PHYSICAL OCEANOGRAPHY IN PARTIAL FULFILLMENT OF THE REQUIREMENTS FOR THE DEGREE OF

MASTER OF SCIENCE IN METEOROLOGY

at the

MASSACHUSETTS INSTITUTE OF TECHNOLOGY

February 15, 1983

Signature of Author _____
Department of Meteorology and Physical Oceanography, February 15, 1983

Certified by _____
Reginald E. Newell, Thesis Supervisor

Accepted by _____
Ronald G. Prinn, Chairman
Departmental Committee on Graduate Studies

The Variability of Precipitation Patterns Over the Central and West Pacific Ocean

by

Kevin J.E. Walsh

Submitted to the Department of Meteorology and Physical Oceanography on February 15, 1983, in partial fulfillment of the requirements for the degree of Master of Science in Meteorology.

ABSTRACT

Empirical orthogonal functions (EOFs) are used to analyze the patterns of rainfall over the Pacific Ocean. The main area of activity is found to be located over the Kiribati region (0 175E), with areas of opposite sign over Australia and over the Caroline Islands (8N 160E). Seasonal maps of the EOF are drawn up, and identifications of the patterns found with large scale features of the atmosphere are made. Correlations are performed between the time series of the first eigenvalue of the EOF of rainfall and a number of other quantities. It is found that there are strong correlations between the EOF of rainfall first eigenvalue time series and indices of the Pacific sea surface temperature, with the rainfall time series lagging the sea surface temperatures by up to three months. There are weaker but still significant correlations between the EOF time series and an index of Australian rainfall, with the Australian rainfall index leading the EOF time series by a month. An index of the strength of the Hadley circulation is observed to lead the EOF time series by a year, while an inverse correlation of the index follows the EOF time series by a season. An hypothesis is made that the center of rainfall activity over Kiribati may be a significant source of energy for the tropical circulation.

Thesis Supervisor: Reginald E. Newell

Title: Professor of Meteorology

TABLE OF CONTENTS

LIST OF FIGURES

15. January precipitation from Taylor (1973), in millimeters.

16. July precipitation from Taylor (1973), in millimeters.

17. Time series of Pacific SST for indicated locations, from Newell (personal communication), in tenths of a degree Celsius.

18. Time series of SST for 0° 165°W, from J. Hsiung (personal communication), in degrees Celsius.

19. Wind anomalies for 0° 160°W, from J. Hsiung (personal communication), in meters per second.

20. January moisture flux divergence.

21. July moisture flux divergence.

22. Temperature variations of SST and free air temperature from Newell (1979).

23. Chronological sequence of events from correlations.

TABLES

CHAPTER ONE

INTRODUCTION

The variations of rainfall over the Pacific Ocean are of crucial importance for a clear understanding of the general circulation. Latent heat release is an important factor in the maintenance of the general circulation, and the largest variations in the tropical atmospheric heating are those due to latent heat release (Webster, 1972). The Pacific Ocean is the largest ocean, and exerts the greatest influence on the atmosphere of any ocean. Since latent heat release is closely associated with rainfall, a study of rainfall patterns and variations over the Pacific would be likely to shed new light on the processes that govern changes in the general circulation.

Of equal importance from a practical basis is the problem of forecasting rainfall in the Pacific and in the surrounding continental areas. The nations that bound the Pacific comprise some of the most densely populated nations on earth. The effects of large variations in the temporal distribution of rainfall in these countries are at times literally matters of life and death. Adequate and steady rainfall is particularly important for the poorer third world nations which operate in large part on a subsistence economy. However, it is also true that for a country such as Australia, which has a marginal climate in many respects

in its northern section (Gentilli (1971)), variations in rainfall can cause the loss of millions of dollars worth of property through the agency of drought or flood. The problem of forecasting is therefore obviously one which has the potential for yielding important results.

As an introduction to the methods used in this paper, it might be worthwhile to review work that has been done on related topics: specifically, the Southern Oscillation, its relation to Pacific and Australian rainfall, and work on Empirical Orthogonal Functions (EOF) of rainfall over the Pacific.

Much work has been done recently on the phenomenon of the Southern Oscillation, which was first thoroughly investigated by Walker (1923-1937). The oscillation is defined as a fluctuation in pressure between the equatorial western Pacific and the southeast Pacific: when the pressure over one area is high, it tends to be lower than the other. A Southern Oscillation index is defined as being positive when pressure is high in the southeast Pacific. Typically, the pressure records of a number of different stations are combined to form an index. For example, one of the most commonly used is the pressure at Tahiti minus the pressure at Darwin. This oscillation seems to have a number of strong effects on the global circulation. Troup (1965) noted that there seems to be an equatorial east-west circulation in the Pacific that is

modulated by the Southern Oscillation (hereafter referred to as the SO). This circulation was named the Walker circulation by Bjerknes (1969). Later authors found such East-West circulations occurred across the globe: Boer and Kyle (1974) found that their presence was not limited to the Pacific alone.

The SO also has effects on the circulation patterns and on sea surface temperatures (SST) in various parts of the globe. Bjerknes and Rowntree (1972) demonstrated that there was a link between the equatorial Pacific and the midlatitudes through the SO. The SO has also been used in a number of studies as a tool to predict the SST in various regions and thereby to predict the rainfall.

The most spectacular change in the SST in the Pacific region is associated with the phenomenon known as El Niño. This is an increase in the SST off the Peru coast which is associated with a number of large-scale changes in the atmospheric circulation. During a period of El Niño, the Walker circulation is much weaker than normal, as shown by Bjerknes and other authors. It is associated with increased rainfall over much of the central and eastern Pacific, and decreased rainfall over the western Pacific. Quinn and Burt (1972) have shown that the SO can be used to predict periods of heavy rainfall over the equatorial Pacific, while Quinn (1974) has shown that the SO can be used to predict the occurrence of El Niños. Donguy and

Henin (1980) noted that the appearance of El Nino in the eastern Pacific was followed by drought in the southwest Pacific.

Other authors have suggested mechanisms for the development of rainfall anomalies over the Pacific area. Wright (1977) suggested that a positive feedback mechanism accounted for the well-known persistence of rainfall anomalies over the central Pacific. Fleer (1981) noted that rainfall in this region was mostly dominated by a multi-year signal, and that the annual cycle was irrelavent to the distribution of rainfall amounts. Nicholls (1981) has also investigated the possibility of positive feedback mechanisms, this time in Indonesia, as a possible long-term prediction tool over that region and over northern Australia.

Northern Australia is an area that has been suggested as a likely region for the study of long-term predictability of rainfall and other climatic variables (Nicholls (1982)). Rainfall over Northern Australia is predominantly governed by the location and intensity of the Inter-Tropical Convergence Zone (ITCZ) during the southern summer. Only certain exposed coastal regions receive significant rain in this area during the southern winter (Gentilli (1971)). Berson (1961) has suggested that the primary factor behind the development of the Australian monsoon is the northern hemisphere winter

intensification and southward extension of the Hadley circulation. However, Kraus (1954) and Troup (1961) also showed that rainfall in the northern section of Australia was negatively correlated with the mean meridional pressure gradient at 200 mb in the southern hemisphere. Pittock (1975) has shown that there is a strong correlation between the SO and Australian rainfall, particularly over the inland subtropics. This conclusion has been confirmed by Stoeckenius (1981), who also noted other teleconnections with the SO in other parts of the globe. Streten (1981) showed that the annual rainfall over northern Australia was related to the SST of the surrounding ocean areas: during wet years, the SST was high, while the opposite was true during dry years. Moreover, Newell *et al.* (1982) showed that teleconnections between the SO and SST for various lag times extended to significant levels across the entire Pacific. Thus it seems reasonable to assume that there are further well-defined relationships between SST patterns in the Pacific and the variations of Australian rainfall.

Since Kidson (1975) has identified the SO with the first eigenvectors of pressure, temperature and rainfall, it might also be assumed that worthwhile results could arise from an examination of the EOF pattern of rainfall over the Pacific. EOFs were first applied to meteorological analysis by Lorenz (1956). Kidson (1975) performed

an EOF analysis of various parameters for the tropics, but only used ten years of data. His data distribution over the Pacific was also poor. This study uses more than twenty years of data, and the best available distribution of stations over the Pacific. To the best knowledge of the author, no EOF study of Pacific rainfall has been done since Kidson's work.

To sum up, the author hopes to demonstrate some relationships between the large-scale fluctuations of the ocean and the atmosphere in the Pacific Ocean, and also to show connections between these fluctuations and the changes in northern Australian rainfall. Using the technique of EOF analysis and by making some physical arguments, it is also hoped that some of the mechanisms which govern these teleconnections can be elucidated.

CHAPTER TWO

DATA AND ANALYSIS

The data for this work was taken from a number of different sources. Monthly rainfall data was taken in part from the *Monthly Climatic Data for the World* published by the WMO. Data was also obtained from the *World Weather Records*. This data was read off and punched in by hand. Other rainfall data was taken from a Pacific rainfall data set compiled by Klaus Wyrtki, a similar data set compiled by John Kidson, and from an atlas of Pacific Rainfall published by Taylor (1973).

The data is of varying quality. Some stations have a number of years of data missing, while others fail to report for individual months. It was decided to exclude from consideration those stations that had more than five percent or so of their data missing over the timespan of the study (1951-1974). This assumption is not based on any statistical analysis of the situation, but it seems to be a reasonable estimate of the number of data points that could be missed without the EOF pattern being seriously affected.

Missing points were excluded from the calculation of the EOF. Normalized deviations from the mean over the period of the study were used. The normalization was accomplished by dividing the deviations by the standard

deviation of the individual month in question, for each station. A seasonal stratification of the EOF was also carried out by including only those points for those months in each season in the calculation.

The geographical distribution of the data set is somewhat uneven (see Figure 1). The most completely covered region is the area near the intersection of the equator and the dateline, where there are a number of small islands of considerable importance to the climatological record. On the other hand, the sparsest region of data is the eastern Pacific Ocean near the equator, where there are no stations at all. Similarly, in the southeast Pacific there is only one station: Easter Island. Another disappointment is the lack of any adequate stations in Indonesia, an important region in that it is one of the primary sources of vertical motion for the Walker circulation. Nevertheless, the station distribution is adequate for the purposes of this study.

Outliers were eliminated by the requirement that any point that was more than 7.0 standard deviations above the mean for that month was to be discarded. Again, while there seems to be no hard and fast rule on such a restriction, inspection of rainfall records indicates that this restriction encompasses all observed variations while leaving room for obviously bad points to be discarded. In addition, much of the data was checked by hand to insure

that such points were either corrected or discarded.

Other EOF studies have often used a slightly different method of approach than that used for this study. The most common method of approach has been to divide the area of study up into a number of grid points and thereby analyze the field by interpolation between existing stations (see for example Craddock and Flood (1969), Kidson(1975) and Arkin(1982). To test to see if the method used in this study is valid, correlations between rainfall at a station near the center of the EOF first eigenvalue main maximum (see Figure 2) and rainfall at all other stations in the data set were performed. The EOF values are defined as the eigenvectors of the variance-covariance matrix of the system (see Appendix). Since this work uses normalized deviations of rainfall, the matrix elements of the variance-covariance matrix are simply the correlation coefficients of each point with itself and every other point in the data set. The test correlation coefficients calculated essentially reproduced the observed EOF pattern. Thus, although slightly different eigenvectors might be produced if the data set had been interpolated to give grid point values, it seems safe to say that the same overall pattern would have been produced.

CHAPTER THREE

RESULTS

(I) EOF Analysis

The first Eigenvalue of the EOF of rainfall accounts for 7.7% of the variance (Fig. 2). The main area of activity of the EOF first Eigenvalue is located in the central west Pacific, in the Kiribati region, on the equator near the dateline. This maximum is counterbalanced by a number of smaller minimums: in the Cook Islands near 20° South 169 degrees West, off the northeast coast of Australia, and in the Pacific North of New Guinea. These are the major regions of oscillation, although there are smaller, less significant minimums over the Hawaiian Islands and near Wake Island.

The pattern of the main center of activity clearly resembles the pattern found by Kidson (1975) (Fig. 3). The only real difference is the extension of the area of positive EOF through Midway Island (28N 177W). There is another region of some slight difference over northeast Australia, where the intensity of the minimum is greater than in Kidson's results, and also over the Cook Islands, where Kidson's zero line is displaced further to the South than in these results. Overall, however, the pattern resembles Kidson's work both in intensity and in geographical location.

As previously pointed out, there is no data in the eastern Pacific on which to base an assumption about the variability in this region. Kidson also had the same difficulty with his analysis. There may be large scale non-seasonal variability in this region, but we have no way of knowing whether this is the case or not. Inspection of data from some partial records of some stations in the Galapagos Islands (1S 90W) does indeed show considerable variability, but it is difficult to say how this variability relates to the calculated EOF of rainfall time series.

The variation in the first eigenvalue EOF pattern from season to season is quite noticeable. The center of activity remains over the central west Pacific year round, but it shifts north and south slightly with the sun. In the northern spring (March-May), (Fig. 4), the main center is located near the equator; major minimums are over northern Australia, and near Guam (13N 144E). In the northern summer (June-August), (Fig. 5), the center of activity shifts slightly northwards, and a distinct minimum develops near Pago Pago (13S 172W). A large area of positive sign extends across the western Pacific into the Phillipines. The Australian minimum is displaced further south, and Darwin (12S 131E) has a positive sign. There is also a large area of positive sign over the Austral Islands (25S 140W).

In the northern autumn (September-November), (Fig. 6), the main center of activity shifts south of the equator, and the large area of positive sign over the Western Pacific vanishes, to be replaced by a strengthening area of negative sign. The Pago Pago minimum observed in the summer weakens, and a new area of low values forms near New Caledonia (21S 166E). The Australian mainland reverts to negative values. The Hawaiian Islands are in a small minimum, as they are year-round. Finally, in the northern winter (December-March), (Fig. 7), the center of activity is located somewhat south of the equator. Major minimums are located across the southwest Pacific from the east of Australia through Fiji (18S 178E) to Rarotonga (22S 160W), and in the northwest Pacific from the southern Phillipines through Guam to the eastern Caroline Islands (8N 160E).

The second eigenvalue, (Fig. 8) which accounts for 5.0% of the variance, shows maximum values over the Austral Islands, and over the Phillipines and the Carolines. The major minimum is over Australia. The main center of activity is over the Phillipines. Comparing the second eigenvalue to Kidson's results, (Fig. 3) there is some agreement. Kidson's main maximum is over the Carolines, with a secondary maximum over the Austral Islands, as in our results. Although his major minimum is over the South Pacific near 30 degrees south 160 degrees west,

this is not significant because of the lack of data in this region. Thus our pattern for the second eigenvalue bears a good resemblance to Kidson's results.

One point to note is the low proportion of the variance accounted for by the first and second eigenvalues. As Kidson points out, this is typical of the smaller scale patterns of rainfall variations, as opposed to the larger scale variations of variables such as temperature and pressure.

EOFs were calculated for other eigenvalues. Craddock and Flood (1969) proposed a method by which the significance of eigenvalues could be determined. Their method was to plot the natural logarithm of an eigenvalue against its ordinal number. The pattern that they obtained for all of their large eigenanalyses resembles that obtained for this study (see Figure 9). They proposed the ad hoc statement that "in meteorology, noise eigenvalues are in geometrical progression", and thus eigenvalues whose plots lie along an approximate straight line may be safely discarded. For our purposes, this would mean that eigenvalues below about number 15 could be dispensed with.

This may be true from a collective standpoint in that the field reproduced from a combination of these eigenvalues may differ only negligibly from the original

field. However, this does not mean that, individually, all the eigenvalues are accurate representations. North et al. (1982) give a rule of thumb for deciding if an EOF pattern is useful. The sampling error $\Delta\lambda$ is defined

$$\Delta\lambda \sim \lambda(2/N)^{1/2}$$

where λ is the eigenvalue and N is the number of points in each time series. The rule is that if two eigenvalues lie within $\Delta\lambda$ of each other, the EOF patterns are subject to mixing errors and are thus not resolved.

Persistence in the time series is accounted for by calculating the autocorrelation function of each time series. The persistence is here loosely defined as the time required for the autocorrelation function to fall below the 95% significance level of the time series. The individual persistences for each station are then averaged to obtain an estimate of the overall persistence.

The average persistence is calculated to be about 1.6 months. To apply this results to North's formula, N is divided by the average persistence to obtain a new figure for the number of truly independent points. In our case (see Table 1), the first four eigenvalues are averaged to obtain

$$\Delta\lambda \sim 1240\ (2/(288/1.6))^{\frac{1}{2}}$$

$$\sim 130$$

The separation between the first, second and third eigenvalues is greater than the sampling error, while the separation between the third and the fourth eigenvalues is less. Thus, the observed EOF patterns for the third and fourth eigenvalues are not likely to be good representations of the true patterns.

The time series of the first eigenvalue (Fig. 10) predictably resembles Kidson's time series, (Fig. 3) over the time period that Kidson used for his study.

(II) Relationships with Other Quantities

Lagged correlations were calculated between the first eigenvalue EOF time series and a number of other significant quantities. The most important quantity for the production of rainfall over the tropical Pacific is likely to be the SST over that region. Therefore, correlations were calculated with an EOF time series of Pacific SST, and with an equatorial zonal mean SST (ZMT).

The EOF time series of Pacific SST (Fig. 11) is taken from data used in Weare, Navato and Newell (1976), supplied by the authors. Non-seasonal variations in the EOF pattern for the SST were extracted from the original data. The data used ran from 1951 to 1973. A table of

correlations of various quantities is seen in Table 2. The correlation of the time series of the first eigenvalue of the EOF of SST with the first eigenvalue of the EOF of rainfall is quite pronounced: the highest correlation is 0.761, with the SST leading the rainfall by one month.

The ZMT data (Fig. 12) was supplied by Dr. A. Navato. The ZMT is defined as the average SST along the meridian 2.5 degrees south from the coast of South America to 140 degrees west. The data is taken from ship reports. The highest correlation occurs for the ZMT leading the rainfall by three months, with a correlation of 0.677. Thus in both cases the SST changes precede the changes in rainfall over the center of activity. The ZMT is a particularly useful indicator in that the temperature across the eastern Pacific at that latitude is a useful indicator of El Nino outbreaks and associated phenomena.

Since northern Australia is in a zone of opposite variability from the center of activity, it was thought useful to examine correlations of the EOF time series with an Australian ranfall index, (Fig. 13) and with individual Australian stations. The Australian rainfall index was calculated by adding the normalized departures from the long-term means of the cube root of rainfall of the eleven Australian stations included in the EOF study, over the period 1951-1974. The cube root of the rainfall was

chosen because rainfall is not normally distributed with time, and thus any index of raw rainfall data might be dominated by high rainfall amounts at one or two points (see, for example, Stidd (1953)). The added cube root normalized departures were then smoothed by taking five-month running means, this being the typical timescale of the "wet" or the monsoon season (December-April) over northern Australia. Strictly speaking, some of the stations included in the index do not have a monsoonal climate, but they are all much wetter during the summer than during the winter.

The results show that the highest correlation between the index and the EOF is -0.419, with the index leading the EOF by one month. This result is significant at the 99% level, if we assume that the smoothing involved in the rainfall index reduces the number of independent points by a factor of five.

If we look at the results of correlations of the EOF with some individual Australian stations, some interesting results emerge. Four stations were correlated (see Table 3). The results show that none of them have as high a correlation as the rainfall index, although they all exhibit the same behaviour in terms of time lag. The time lags range from almost a contemporary correlation in the case of Darwin (94120) to lags of two months, with the rainfall preceding the EOF, in the case of

Mackay (94367) and Brisbane (94578).

Since the rainfall over northern Australia is heavily seasonal, it might be worthwhile to examine correlations over just the period of the monsoon (December-April). The EOF was monsoonally stratified: that is, only the monsoon months were included in the calculation. The Australian rainfall index was also taken for these months. The results (Table 4) show the same behaviour as already observed: The rainfall index leads the EOF by one month, with a correlation of -0.438.

The large scale variations observed in the tropics might be expected to influence the mid-latitudes. Accordingly, figures were obtained for the meridional temperature gradient in the mid-latitudes (Fig. 14) in the following manner. The seasonal values for the geopotential difference between the surface and 100 mb for the tropics (30N-30S) and temperate regions (30°-60°) were obtained from the data set used by Angell and Korshover (1978). To obtain a measure of the meridional temperature gradient in each hemisphere, the individual seasonal values for the temperate regions in each hemisphere were subtracted from the individual values for the tropics. Thus if the geopotential difference between the surface and 100 mb is large in the tropics and small in the temperate regions, a large meridional temperature gradient at low levels is implied.

The results (Table 2) show that there is a definite, although not automatic, relationship between the intensity of rainfall in the central west Pacific and the meridional temperature gradients. Highest leading correlation of the seasonally averaged EOF with the southern hemisphere temperature gradient is 0.344, with the rainfall leading the gradient by one season. The correlation with the northern hemisphere gradient is comparable, with the highest leading correlation being at a lag of one season also, at 0.320. Both of these correlations are significant at the 99% level, although the percentage of the variance explained is comparatively small. If the gradients in both hemispheres are added to obtain a value for the total gradient, the same behaviour is observed: a leading correlation of 0.374, with the rainfall leading the gradient by one season.

One interesting aspect of these results is the existence of the maximum correlation in the temperature gradients about a year before the rainfall variations. This correlation is in all cases stronger than the leading correlation. This may possibly indicate some mid-latitude influence on the sequence of events which trigger the El Niño. In all of these results, however, the amount of the variance explained is low, and it would be difficult to make firm conclusions about these influences.

CHAPTER FOUR

INTERPRETATION OF RESULTS

(I) Interpretation of EOF Patterns

As an aid in interpreting the EOF patterns, Taylor's (1973) rainfall atlas was used to find areas of agreement between patterns of the first eigenvalue of EOF of rainfall (Fig. 2) and the actual large scale features that are seen in the atmosphere. The large area of maximum EOF intensity over the Pacific may be identified with a long dry tongue on Taylor's map extending westwards along the equator. The large positive area over the southwest Pacific in the EOF pattern may be identified with the South Pacific Convergence Zone. Similarly the maximum in the ITCZ over the Carolines may be identified with a similar positive area in the EOF pattern.

Comparing the summer and winter EOFs with Taylor's July and January maps, (Figs. 15 and 16) we find that in Taylor's maps, the large area of low precipitation is much further west in July in the equatorial region than in January. Similarly, the large EOF maximum in the central Pacific is much further west in July than in January. The agreement with the SPCZ is not as clear, as there is an area of negative activity over Samoa in July that does not correspond to an area of high rainfall, but rather to an area of low rainfall. In any event, the main indications of the EOFs are in terms of variability: a positive

area has high rainfall when a negative area has low rainfall. One clear indication of the northern winter EOF is that the entire southwest Pacific region, with the exception of New Zealand, has low rainfall during the southern summer when the area near Kiribati has high rainfall. This confirms the results, among others, of Donguy and Henin (1980), who noted that El Nino years correspond to drought conditions in the southwest Pacific, since most of the rain in this region occurs in the southern summer. The same pattern is also true for the northern spring EOF.

(II) Atmosphere-Ocean Interactions

The ZMT is observed to lead the EOF of SST by two months and the EOF of rainfall by three months. A possible explanation for this result is the fact that mid-latitude contributions to the EOF of SST time series play an important part, as Weare *et al.* (1976) note in their discussion of their results. The lag between the EOF of SST and the EOF of rainfall is understandable in terms of a geographical lag from the area of ZMT maximum in the eastern Pacific to the area of maximum rainfall activity in the central Pacific. If we take the typical velocity of westward flowing ocean currents in the region to be 60 cm/sec (Picard (1979)), then for an SST anomaly to travel about 7000 km from the center of ZMT activity

(110W) to the center of rainfall activity (180°) would take approximately 110 days, or close to the observed three-month lag in the correlations.

If we look at some observed SST anomaly propagation patterns, we see approximately the same propagation time. Using figures from Newell (personal communication) and SST data supplies by J. Hsiung (see Figures 17 and 18), we find that the average propagation time from the center of the ZMT activity to the center of activity of rainfall near the dateline is approximately three months.

Julian and Chervin (1978) note that the strength of the South Equatorial Current is inversely related to the SST anomalies over the eastern central Pacific (5N-5S, 80W-180). The South Equatorial Current is a cool current, and when it weakens, the advection of cold water into the eastern Pacific apparently diminishes, and the water in this region starts to heat up. Presumably, this would tend to support Bjerknes' feedback hypothesis. The hypothesis in part is that increased rainfall over the Pacific, caused by higher SSTs, leads to latent heat release and a stronger Hadley circulation, which leads to stronger trade winds at the surface, which in turn leads to lower SSTs, and so on, a negative feedback process. This hypothesis is supported by Reiter (1978), who notes the very strong contemporary correlation between central equatorial Pacific rainfall and the strength of the equatorward

meridional components of the Pacific trade winds. However, Wyrtki (1975) states that there is no evidence for weaker trade winds in the eastern Pacific, and that strong trade winds in the central Pacific cause a buildup in sea level over this area. When these winds relax, Wyrtki says, the accumulated water flows eastward as an internal wave and creates a thicker layer of warm water off Peru, which prevents upwelling.

As a further test of this theory, wind data for the central Pacific supplied by J. Hsiung for the point 160W 0N (Figure 19) was compared with the ZMT. From inspection, there seems to be some relationship between the strength of the zonal wind at this location, although it is far from unequivocal. This theory is still debatable (see Newell (1979)).

The choice of this point is significant in that it is normally located in a region of divergence, south of the Line Islands. Surface moisture flux divergence maps were calculated by the author under the following assumptions. The surface air moisture content q was taken from Weare *et al.* (1980). The 10 m wind v was taken to be characteristic of the entire surface layer, from 1000 to 900mb. The winds were obtained from Klaus Wyrtki. The moisture flux divergence is defined as

$$\nabla \cdot Q_{surface} = \frac{1}{R\cos\phi}\left[\frac{\partial Q_\lambda}{\partial \lambda} + \frac{\partial (Q_\phi \cos\phi}{\partial_\phi}\right]$$

where $Q_\lambda = \frac{1}{g}\int qu\,dp$

and $Q_\phi = \frac{1}{g}\int qv\,dp$

The surface moisture flux should give a good indication of the moisture sources and sinks over the ocean, because there is little in the way of low level stratiform precipitation over the equatorial Pacific. Moreover, Cornejo-Garrido and Stone (1977) found that increased precipitation in the western Pacific is likely caused by moisture convergence, and that this area of convergence corresponds to an area of low evaporation, and thus is a moisture sink. Similarly, the less cloudy southeast Pacific is a moisture source.

The results (see Figures 20 and 21) show a similar pattern to Figures 15 and 16. During El Nino years, the region near the point taken for Figure 19 shows westerly anomalies and typically much higher rainfall than normal. During non-El Nino years, this area shows easterly anomalies and much reduced rainfall. One would expect that these easterly anomalies would pump moisture westwards, perhaps to Indonesia and the Carolines, and perhaps ultimately to Australia. This may be one reason why those areas are out of phase with the main center of activity of the EOF of rainfall.

To digress for a moment, one interesting fact about the area of high EOF variability is the enormous amount of energy that is put into the atmosphere during El Nino conditions in this area. Rao *et al.* (1976) have compiled an atlas of ocean rainfall estimates from satellite measurements. They supply a map of rainfall intensities

for January 1973 (an El Niño year) and January 1974 (a non-El Niño year). If we assume that the main area of rainfall variation is between 157.5E-157.5W and 8N-8S, and that this variation continues for six months, a typical timescale for wet periods over this region, we obtain a total extra latent heat release over this area of about 1.3×10^{24} Joules. Newell (1979) gives data for the change in tropospheric free air temperature (Figure 22). Typically, it can be seen that changes in the free air temperature over a timescale of one year are about 1.7 degrees C. The latent heat release over the central Pacific corresponds to a heating variation for the atmosphere from 3km-10km over the global strip 20N-20S of about 2.1 degrees C. Therefore clearly, if only from energy considerations, it is possible that this area could modulate the non-seasonal behaviour of the tropospheric free-air temperature as a whole.

(III) Connections to Australian Rainfall

The main problem to explain with the results of correlations with Australian rainfall is the tendency of the Australian rainfall index to precede the full establishment of the EOF pattern of rainfall by approximately one month. One clue to this result might be that northern Australian stations tend to precede the EOF less than southern stations as shown in Table 3. Darwin, in the

extreme north of the country, has an almost contemporary correlation with the EOF. One explanation for this result could be that the more southerly stations are more influenced by the mid-latitudes, and thus in some sense are less "pure" than the far northern stations.

One other point to note is that the Indonesian region substantially influences rainfall over northern Australia (Nicholls (1982)). Thus the rainfall regime over Australia is not a simple function of rainfall over the central Pacific, and other influences are undoubtedly at work here.

(IV) Mid-latitude Connections

The results shown here for correlations between the EOF of rainfall and the meridional temperature gradients offer some tentative support to Bjerknes' hypothesis. The release of latent heat over the central Pacific is shown to result in a stronger Hadley circulation one season later. In addition, a weak Hadley circulation is seen to precede the establishment of a high ZMT (Figure 23). Unfortunately, the correlations are low. In particular, it would seem unrealistic to assume that it would take as much as three seasons for a weakened Hadley circulation to results in a high ZMT.

Investigations by Barker (1982) have shown that the establishment of a high ZMT precedes the establishment of

high global relative angular momentum (RAM), another measure of the strength of the Hadley circulation, by one month. The RAM is defined, from Newell *et al.* (1972):

$$RAM = \frac{2\,a^3}{g} \int_0^{p_o} \int_{\phi_1}^{\phi_2} [\bar{u}] \cos^2\phi \, d\phi \, dp$$

One problem with our seasonal averages of meridional temperature is that they are just that: seasonal, and not monthly. Finer scale variations are therefore lost. In addition, the meridional temperature gradient is not measuring exactly the same phenomenon as the RAM. Obviously closer analysis of this problem is required.

CHAPTER FIVE

CONCLUSION

The author has completed a comprehensive study of the EOF patterns of rainfall over the Pacific, and indentified the major centers of activity. The author has also demonstrated a close relationship between the time series of the EOF of rainfall pattern and the time series of the EOF of SST in the Pacific. A close relationship between the EOF of rainfall and the Pacific equatorial ZMT was also shown. A firm relationship between the EOF of rainfall and an index of northern Australian rainfall was demonstrated, and a more tentative relationship was found between the EOF of rainfall and the intensity of the Hadley circulation, a relationship that requires further study.

Promising areas for future research include investigations of moisture fluxes from the Kiribati area across to Indonesia as a possible mechanism for increased Indonesian rainfall and possibly Australian rainfall; a closer study of the mechanisms that govern the strength of the South Equatorial Current as a possible predictor of El Nino; and a closer study of the energetics of the variations of latent heat release over the Kiribati area and over Indonesia as possible "engines" for the tropical circulation.

ACKNOWLEDGEMENTS

The author would like to thank Isabelle Kole, who prepared some of the figures for this manuscript, Liz Manzi, who typed it and prepared other figures, and Susan Ary, who helped with the data processing. The author would also like to thank Diana Spiegel for help with the computations, Jane Hsiung and Dr. Alfredo Navato for consultations, and above all, Professor Reginald Newell for help and guidance.

APPENDIX

EOF ANALYSIS

Following an analysis by Verstraete (1978), it is claimed that the rationale for the use of Empirical Orthogonal Functions is that one wants to find a series of linear combinations of functions that carry a large portion of the variance of the original data set without being redundant or subject to mixing errors. We define a matrix of observations X_{ij} at location I and time J:

$$X = \begin{pmatrix} X_{11} X_{12} \cdots X_{1p} \\ X_{21} \\ \vdots \\ X_{m1} \quad \cdots X_{np} \end{pmatrix}$$

where N is the number of stations and p is the number of different time observations. Suppose there exist two matrices Y and Z such that

$$X = YZ \quad \ldots(1)$$

$$\text{where} = yy^{1} = I$$

$$ZZ^{1} = D \quad \ldots(2)$$

and I is the identity matrix and D is a diagonal matrix. Transposing (1), we obtain

$$X^{1} = Z^{1}Y^{1} \quad \ldots(3)$$

multiplying (1) and (3) gives

$$XX^{1} = YZZ^{1}Y^{1} = YDY^{1}$$

$$\text{Since } YY^{1} = I$$

$$Y^{1}XX^{1}Y = D$$

Y is therefore found by solving the eigenvalue problem. The rows of Y are the eigenvectors of the matrix XX^{1}, and the corresponding diagonal elements of D are the associated eigenvalues. If X is a matrix of deviations $X_{kj} - \bar{X}_i$ where $\bar{X}_i$ is the long-term mean value of the field X at point I, XX^{1} is the variance-covariance matrix of the system. In addition, it can be proved that

$$tr(XX^{1}) = tr(D)$$

which implies that the sum of the eigenvalues d_i is equal to the total time-variance of the data set.

These eigenvalues can be ranked in terms of the amount of variance explained, with the first eigenvalue becoming the eigenvalue that explains the largest proportion of the variance.

REFERENCES

Angell, J.K. and Korshover, J., 1978; "Global Temperature Variation, Surface -100 mb: An Update into 1977." Mon. Wea. Rev. 106, 755-770.

Arkin, P.A., 1978; "The Relationship Between Interannual Variability in the 200 mb Tropical Wind Field and the Southern Oscillation." Mon. Wea. Rev. 110, 1393-1404.

Barker, C.L., 1982; "Variation in Tropical Wind Patterns (1968-1979)." Master's Thesis, Massachusetts Institute of Technology, 56 pp.

Berson, F.A., 1961; "Circulation and Energy Balance in a Tropical Monsoon." Tellus 13, 472-485.

Boer, G.J. and Kyle, A.C., 1974; "Cloudiness, precipitation and vertical motion." Chapter 9 of Vol. 2 The General Circulation of the tropical Atmosphere and Interactions with Extratropical Latitudes. R.E. Newell, J.W. Kidson, D.G. Vincent and G.J. Boer, MIT Press, Cambridge, MA, 371 pp.

Bjerknes, J., 1969; "Atmospheric Teleconnections from the Equatorial Pacific." Mon. Wea. Rev. 97, 163-172.

Cornejo-Garrido, A.G., and Stone, P.H., 1977; "On the Heat Balance of the Walker Circulation." Jour. Atmos. Sci. 34, 1155-1162.

Craddock, O.M and Flood, C.R., 1969; "Eigenvectors for representing the 500 mb geopotential surface over the Northern Hemisphere." Quart. J.R. Met. Soc. 95, 576-593.

Donguy, J.R. and Henin, C., 1980; "Climatic Teleconnections in the Western South Pacific with El Nino Phenomenon." Jour. Phys. Ocean. 10, 1852-1958.

Fleer, H.E., 1981; "Teleconnections of rainfall anomalies in the tropics and subtropics." Chapter 1 of Monsoon Dynamics, ed. J. Lighthill and R.P. Pierce, Cambridge University Press.

Gentilli, J., 1971; Climates of Australia and New Zealand, ed. J. Gentilli. Elsevier Publishing Company, 405 pp.

Julian, P.R. and Chervin, R.M., 1978; "A study of the Southern Oscillation and Walker Circulation Phenomenon." Mon. Wea. Rev. 106, 324-330.

Kidson, J.W., 1975; "Tropical Eigenvector Analysis and the Southern Oscillation." Mon. Wea. Rev. 103, 187-196.

Kraus, E.G., 1964; "Secular changes in the rainfall regime of southeast Australia." Quart. J. Roy. Met. Soc. 80, 591-601.

Lorenz, E.N., 1956; "Empirical Orthogonal Functions and Statistical Weather Prediction." Sci. Rep. No. 1. Contract AF19-(604) 1566, AFCRC-TN-57-256, Dept. of Meteor., MIT, 49 pp.

Monthly Climatic Data for the World, U.S. Department of Commerce, Washington.

Newell, R.E., 1979; "Climate and the Ocean." American Scientist 67, 405-416.

Newell, R.E.; Kidson, J.W.; Vincent, E.G., and Boer, G.J.; The General Circulation of the Tropical Atmosphere and Interactions with Extratropical Latitudes, 1 and 2, 1972 and 1974, The MIT Press, pp. 258-371.

Newell, R.E.; Selkirk, R, and Ebisuzaki, W., 1982; "The Southern Oscillation: Sea Surface Temperature and Wind Relationships in a 100-year Data Set." Submitted to J. of Climatology.

Nicholls, N., 1981; "Air-Sea Interaction and the Possibility of Long-Range Weather Prediction in the Indonesian Archipelago." Mon. Wea. Rev., 109, 2435-2443.

Nicholls, N., 1982; "Prospects for Empirical Long-Range Weather Prediction." Paper prepared for presentation at WMO-CAS/JSC Expert Study Meeting on Long-range Forecasting, Princeton, U.S.A., 1-4 December 1982.

North, G.R.; Bell, T.L.; Cahalan, R.F., and Moeng, F.J., 1982; "Sampling Errors in the Estimation of Empirical Orthogonal Functions." Mon. Wea. Rev. 110, 699-706.

Picard, G.L., 1979; Descriptive Physical Oceanography, Pergamon Press, 233 pp.

Pittock, A.B., 1975; "Climatic change and the Patterns of Variation in Australian Rainfall." Search 6, 498-504.

Quinn, W.H., 1974; "Monitoring and Predicting El Nino Invasions." Jour. Appl. Met. 13, 825-830.

Quinn, W.H., 1972; "Use of the Southern Oscillation in Weather Prediction." Jour. Appl. Met. 11, 616-628.

Rao, M.S.V.; Abbott, W.V., III; Theon, J.S., 1976; Satellite-Derived Global Oceanic Rainfall Atlas (1973 and 1974) National Aetonautics and Space Administration, Washington, D.C.

Reiter, E.R., 1978; "Long-Term Wind Variability in the Tropical Pacific, Its Possible Causes and Effects." Mon. Wea. Rev. 106, 324-330.

Rowntree, P.R., 1972; "The influence of tropical east Pacific Ocean temperatures on the atmosphere." Quart. J.R. Met. Soc. 98, 290-321.

Stidd, C.K., 1953; "Cube-root-normal Precipitation Distributions." Transactions, American Geophysical Union, 34, 31-35.

Stoeckenius, T., 1981; "International Variations of Tropical Precipitation Patterns." Mon. Wea. Rev. 109, 1233-1247.

Streten, N.A., 1981; "Southern Hemisphere Sea Surface Temperature Variability and Apparent Associations with Australian Rainfall." J. Geophys. Res. 86, 485-496.

Taylor, R.C., 1973; An Atlas of Pacific Islands Rainfall, Data Report No. 25, Contract N00014-70-A-0016-0001, Office of Naval Research.

Troup, A.J., 1961; "Variations in upper tropospheric flow associated with the onset of the Australian summer monsoon." Indian J. Geophysics 12, 217-229.

Troup, A.J., 1965; "The Southern Oscillation." Quart. J. Roy. Met. Soc., 61, 490-506.

Verstraete,M., 1978; "Empirical Orthogonal Functions: the method and its applications." Internal Memorandum, MIT, 11 pp.

Walker, G.T., 1923; India Meteor. Dept. Mem 24, 75-131.

_____, 1924; India Meteor. Dept. Mem 24, 275-332.

_____, 1928; Mem. Roy. Meteor. Soc. 2, 97-134.

_____, 1930; Mem. Roy. Meteor. Soc. 3, 81-85.

_____, 1932, Mem. Roy. Meteor. Soc. 4, 53-84.

_____, 1937; Mem. Roy. Meteor. Soc. 6, 119-139.

Weare, B.C.; Navato, A.R., and Newell, R.E., 1976; "Empirical Orthogonal Analysis of Pacific Sea Surface Temperatures." Long-term Climatic Fluctuations: Proceedings of the WMO/IAMAP Symposium, Geneva, 1975 p. 167-174.

_____; Strub, P.T., and Samuel, M.O., 1980; Marine Climate Atlas of the Tropical Pacific. Contributions to Atmospheric Science No. 20. Department of Land, Air and Water Resources, University of California.

Webster, P.J., 1972; "Response of the atmosphere to local, steady forcing." Mon. Wea. Rev., 100, 518-541.

World Weather Records, U.S. Department of Commerce, Washington.

Wright, P.B., 1977; "Effects of Quasi-Biannial Oscillation and the Southern Oscillation on the northern hemisphere circulation." Tellus, 29, 275-279.

_____, 1977; "Persistence of rainfall anomalies in the central Pacific." Nature 277, 371-374.

Wyrtki, K., 1975; "El Nino-the dynamic response of the equatorial Pacific Ocean to atmospheric forcing." J. Phys. Oceanogr., 5, 572-584.

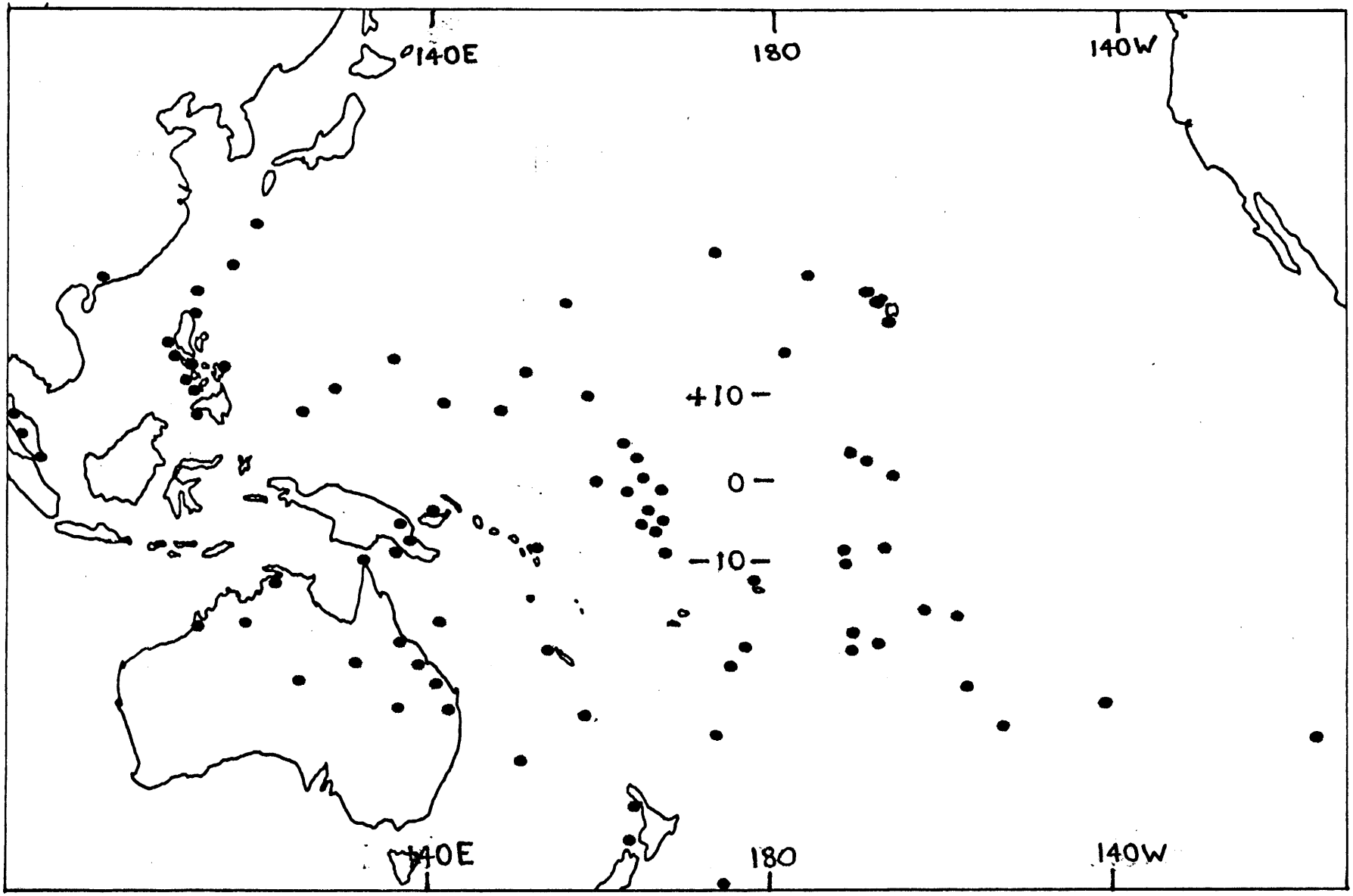

Figure 1. Station Distribution

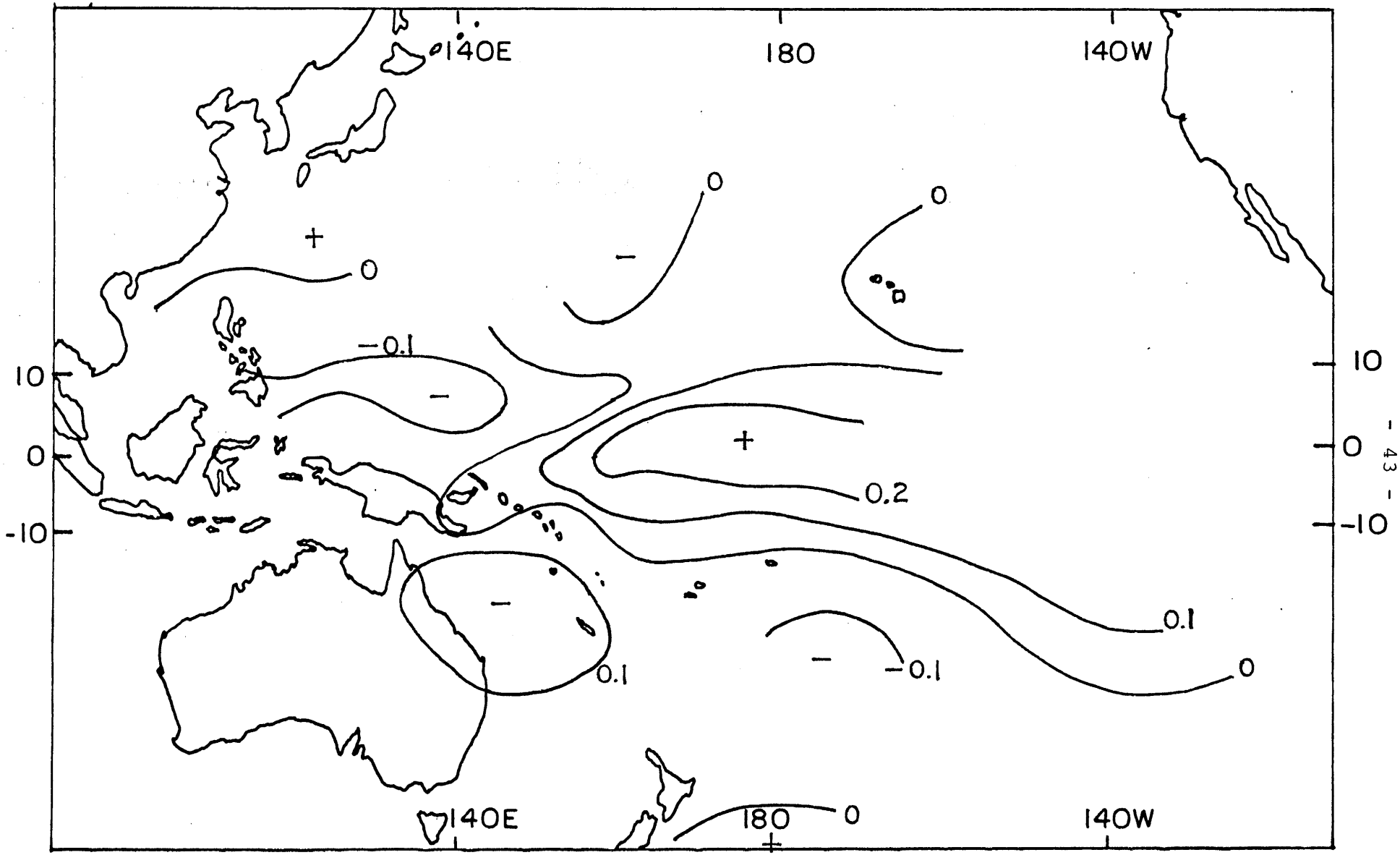

Figure 2. The first eigenvalue of the EOF of rainfall (1951-1974)

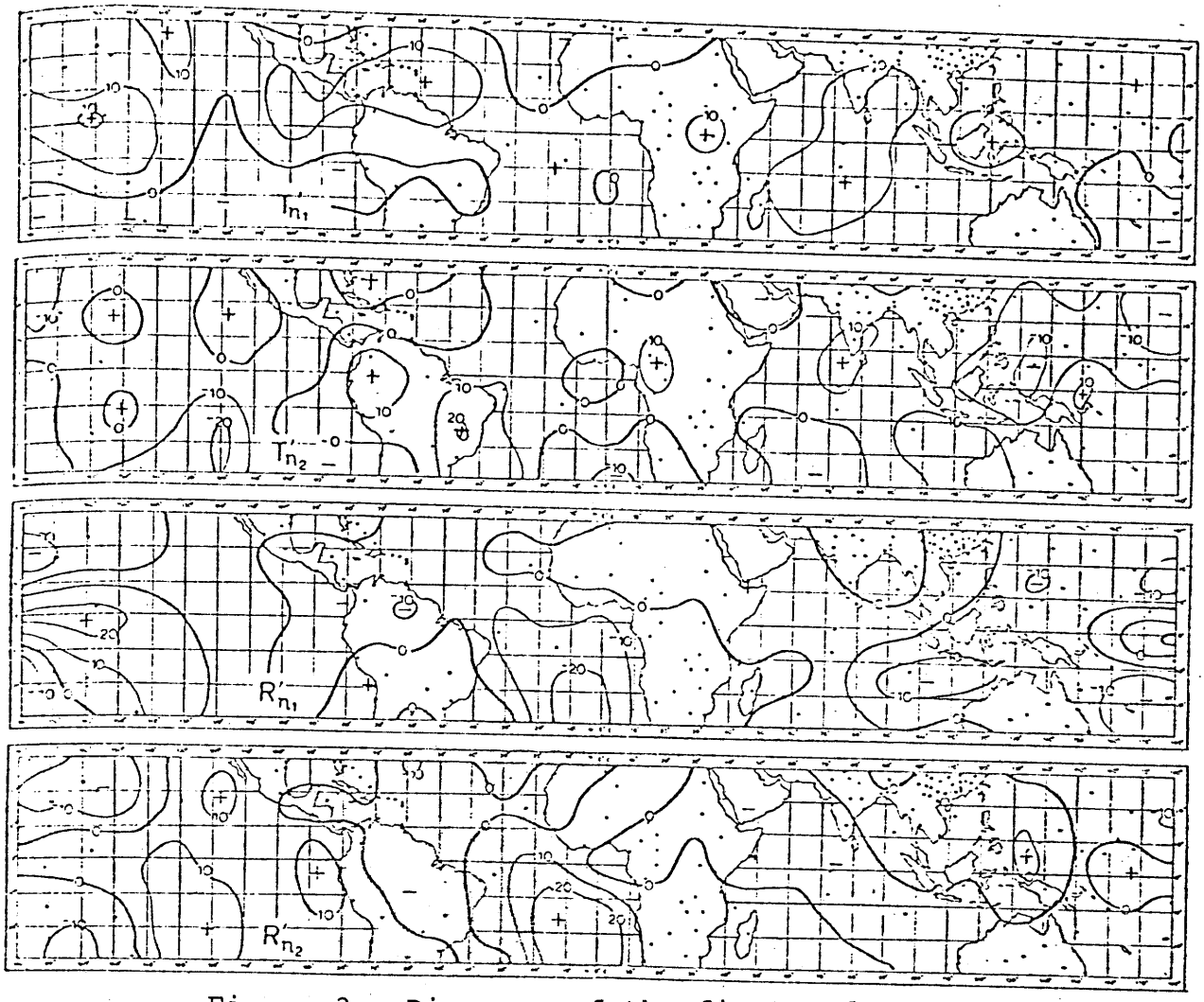

Figure 3. (top) Diagrams of the first and second eigenvalues of normalized departures of temperature and rainfall;

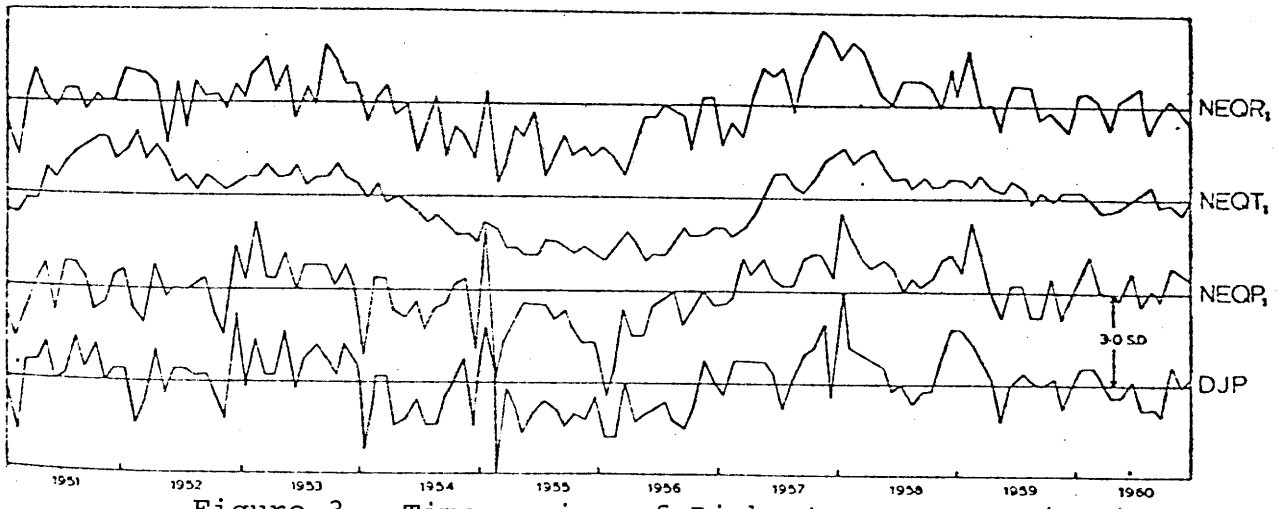

Figure 3. (bottom) Time series of Djakarta pressure (DJP) and the first component of the normalized departures of pressure (NEQP$_1$), temperature (NEQT$_1$) and rainfall (NEQR$_1$), from Kidson (1975).

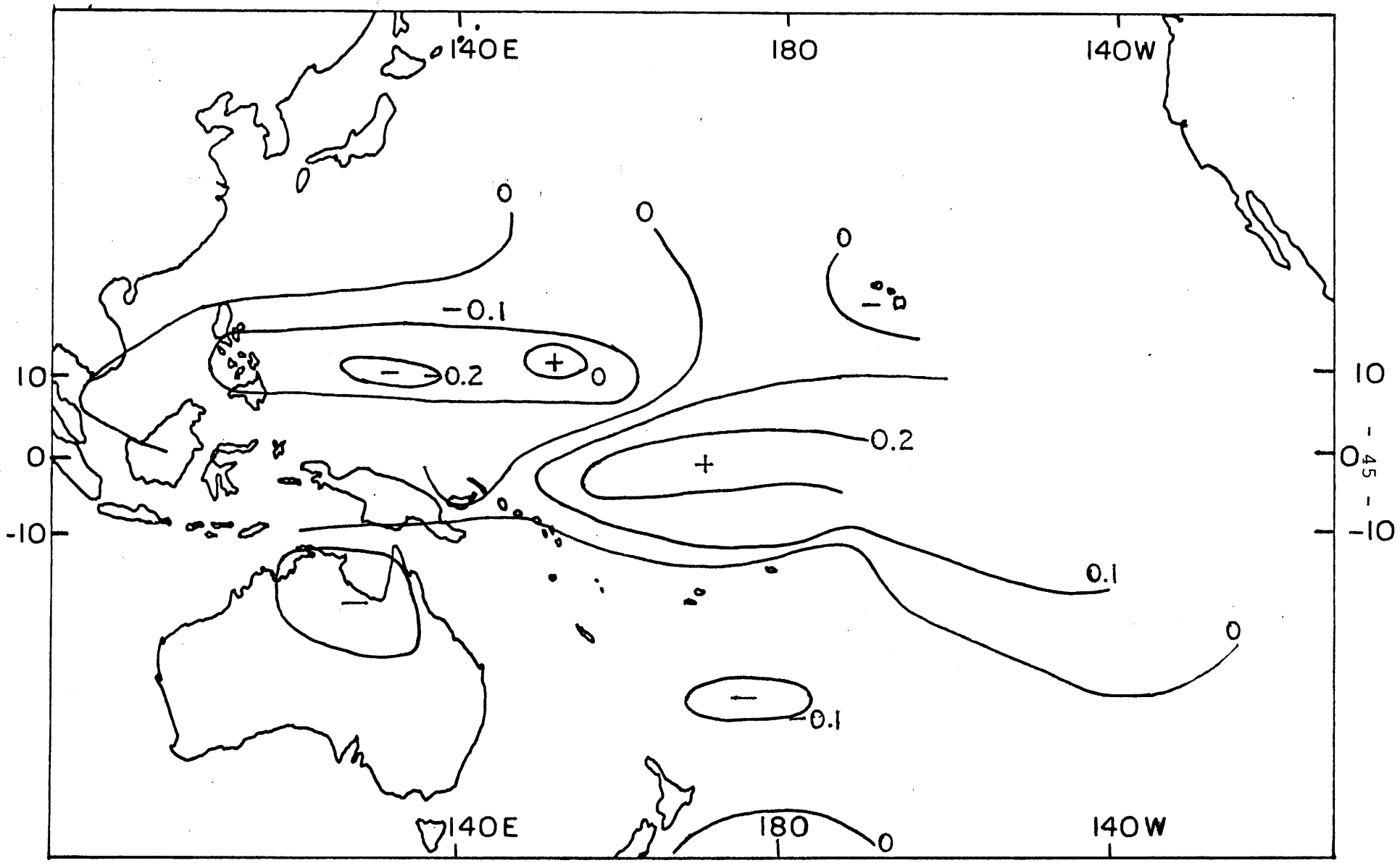

Figure 4. First eigenvalue of EOF of rainfall: spring (1951-1974).

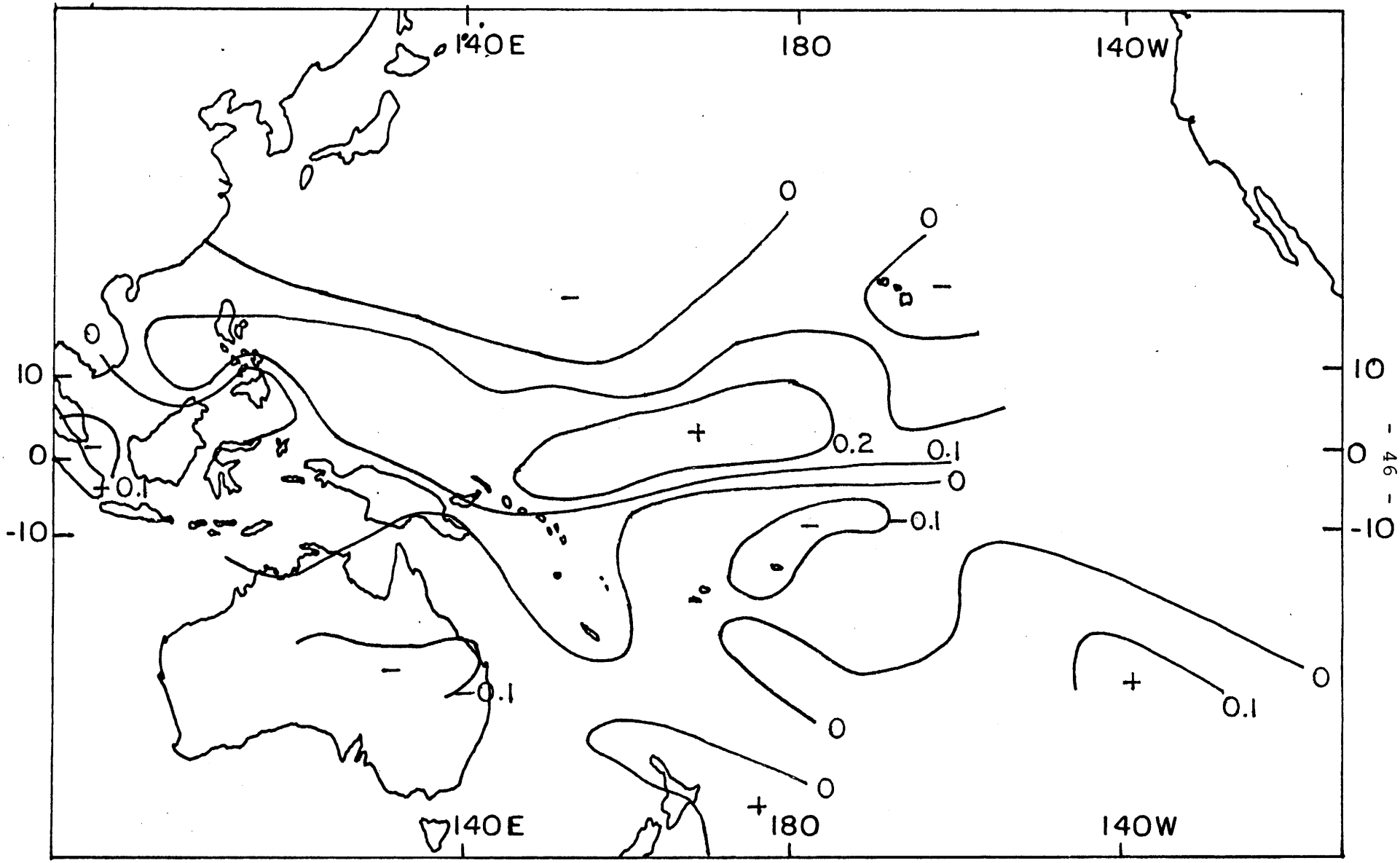

Figure 5. First eigenvalue of EOF of rainfall: summer (1951-1974).

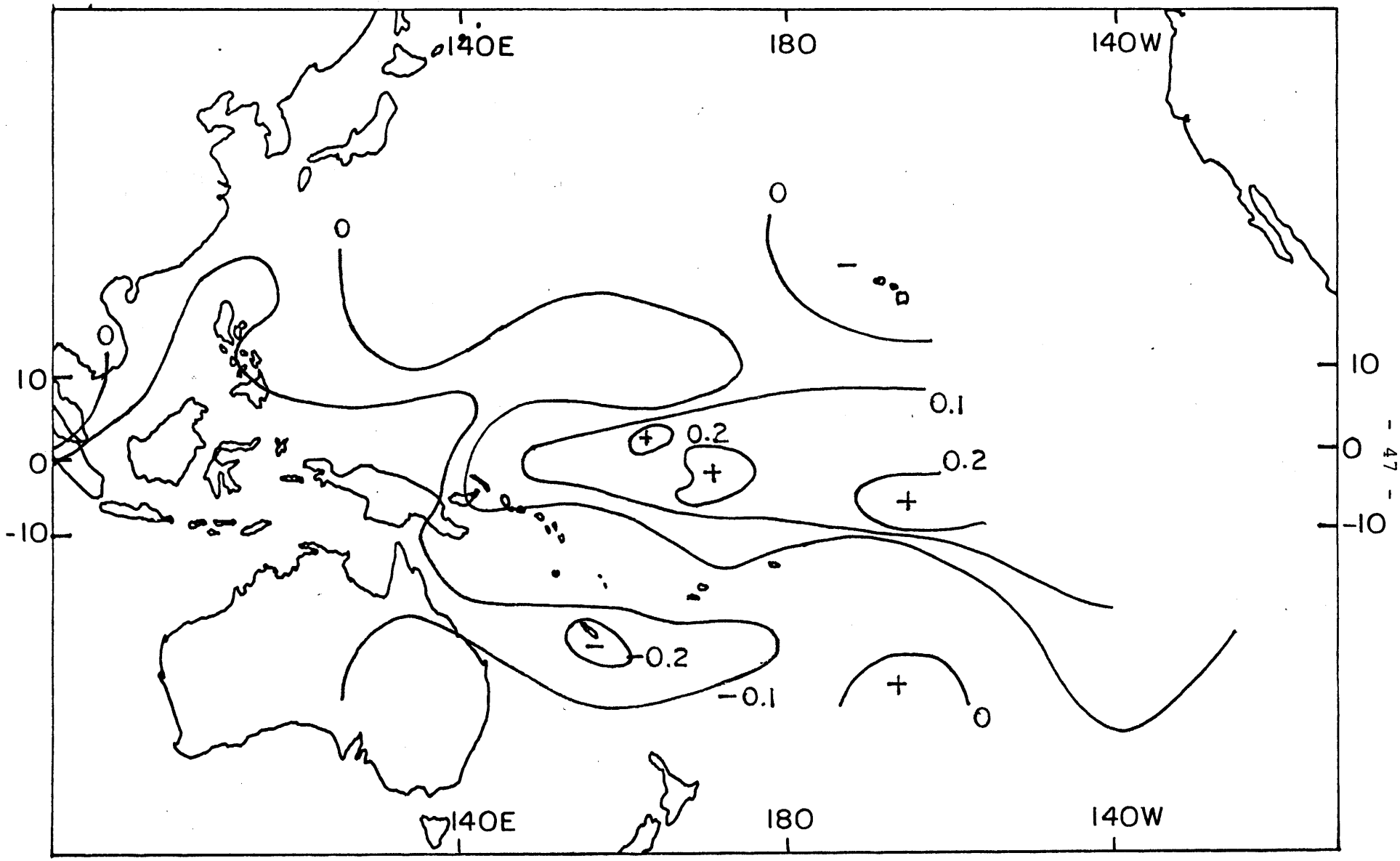

Figure 6. First eigenvalue of EOF of rainfall: autumn (1951-1974).

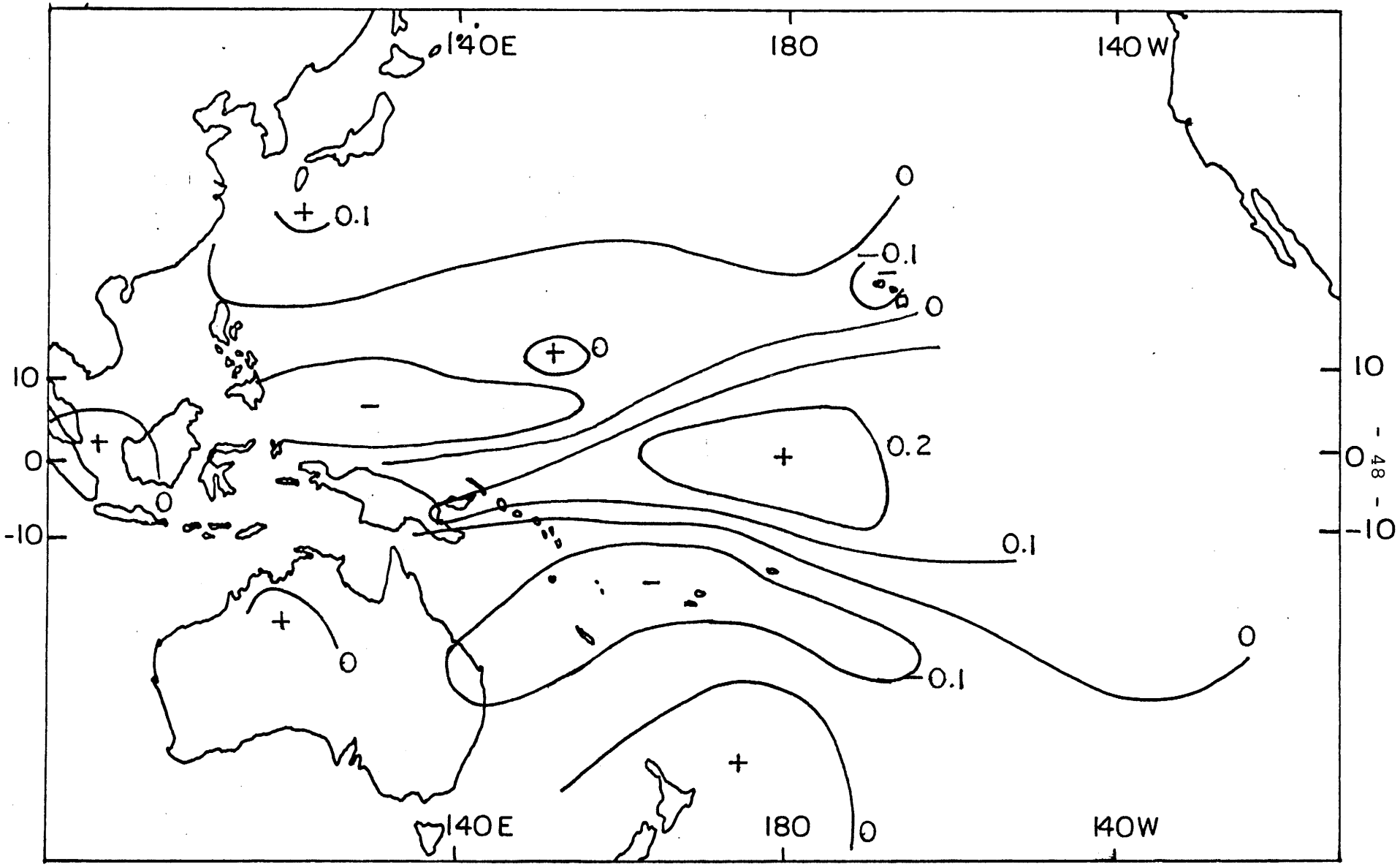

Figure 7. First eigenvalue of EOF of rainfall: winter (1951-1974).

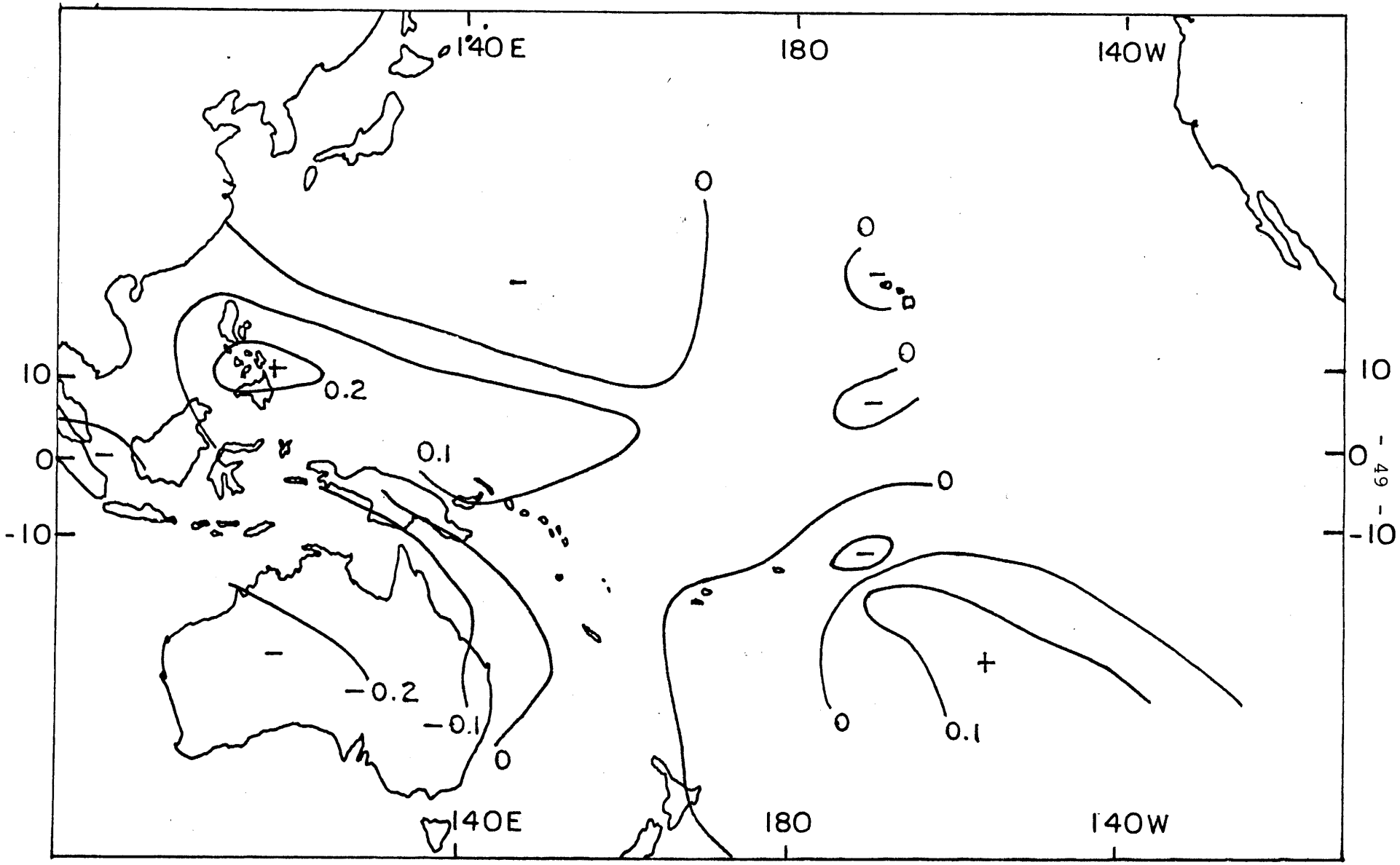

Figure 8. Second eigenvalue of EOF of rainfall (1951-1974).

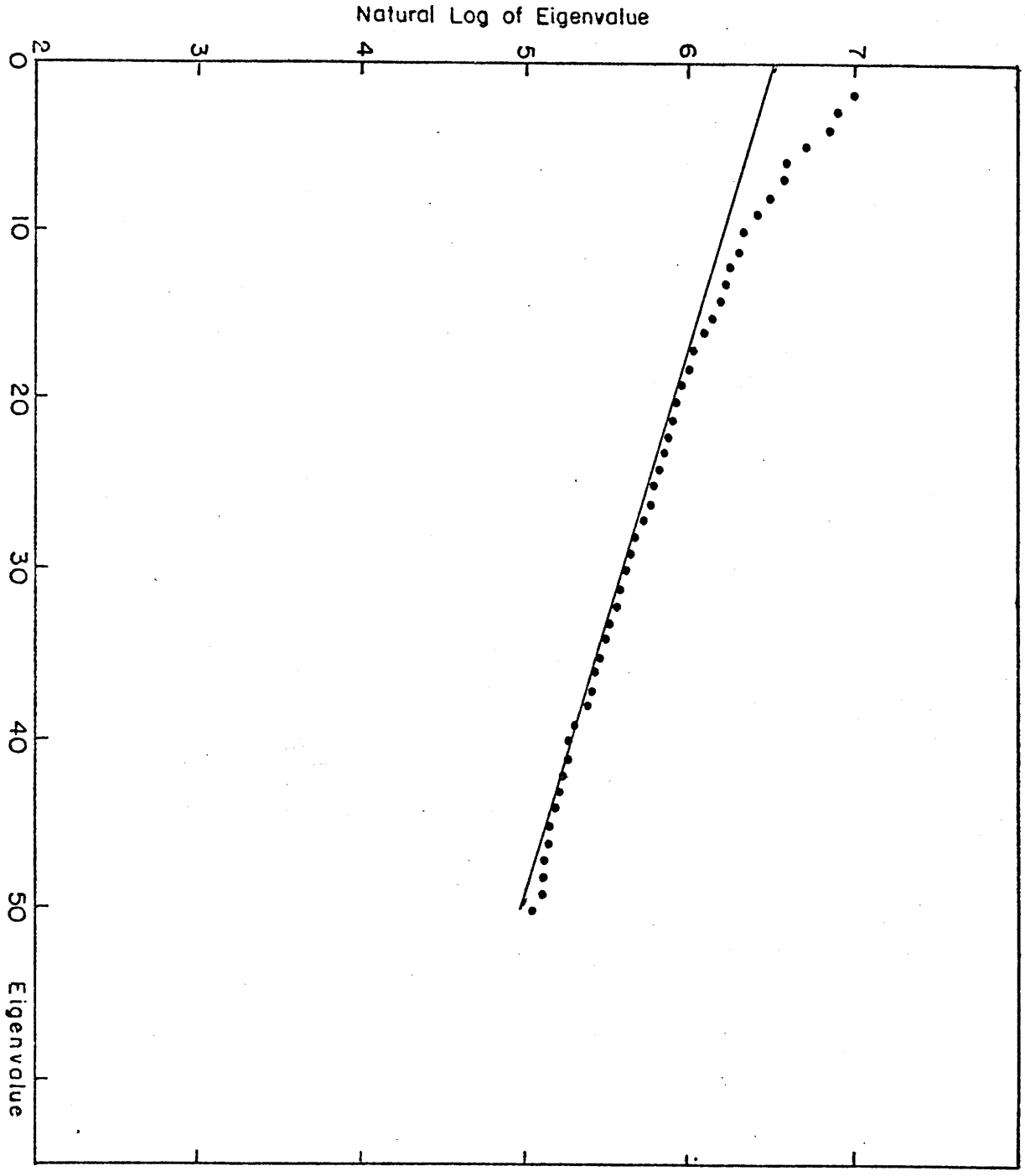

Figure 9. Plotted values of the natural log of eigenvalue versus ordinal number for the first 50 eigenvalues.

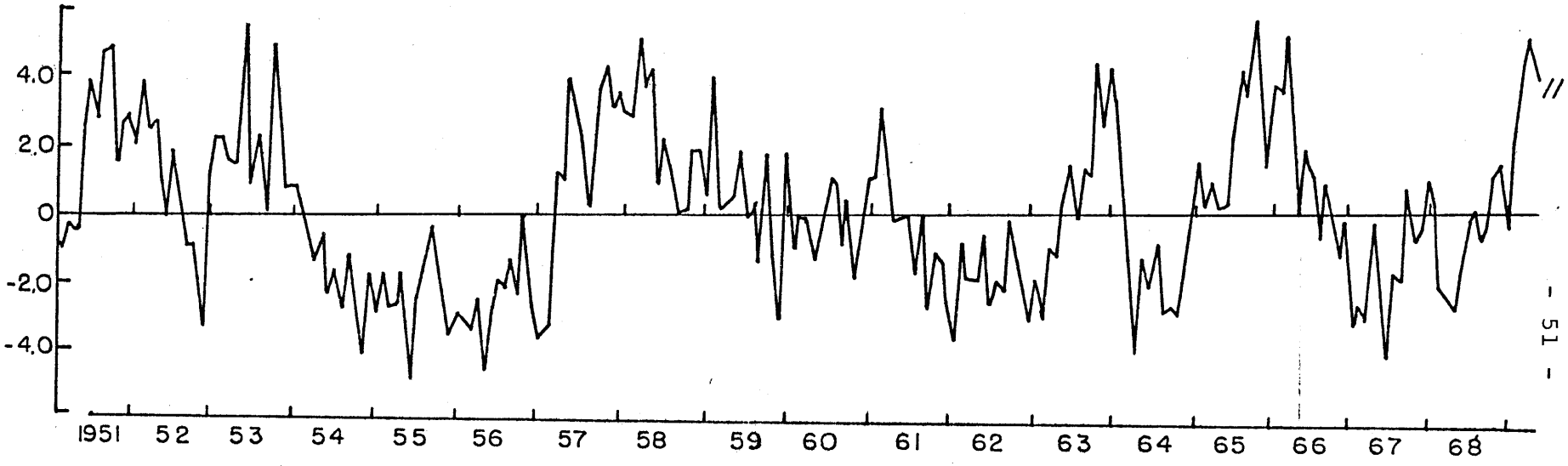

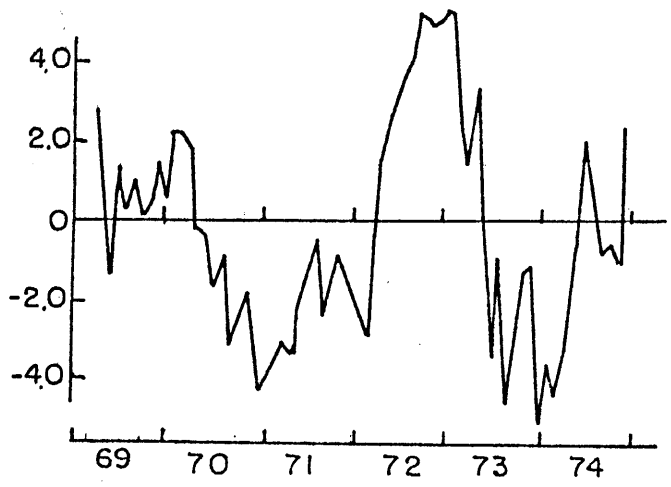

Figure 10. Time series of the first eigenvalue of EOF of rainfall.

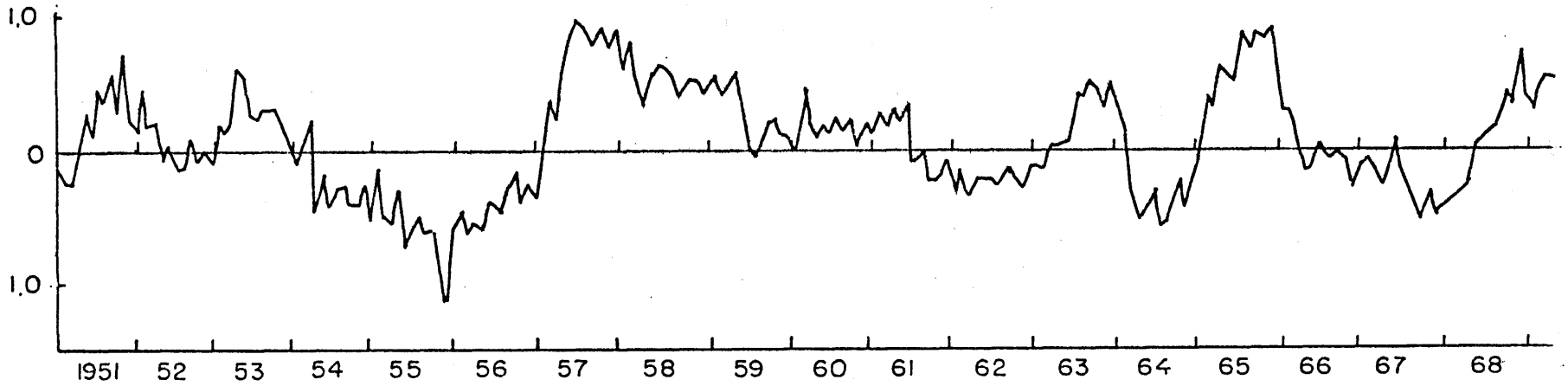

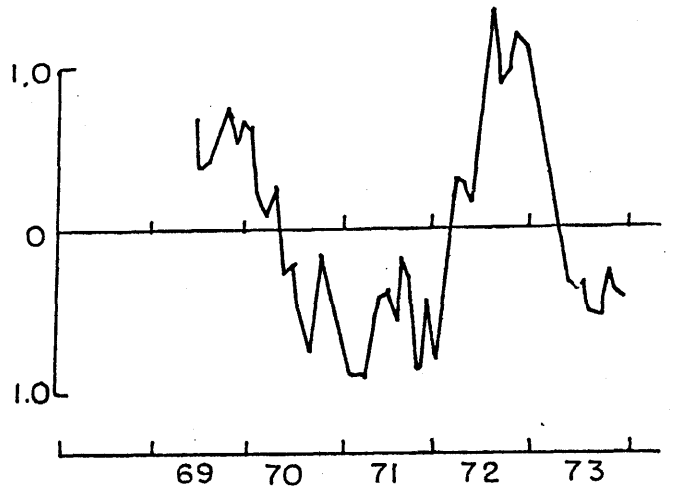

Figure 11. Time series of the first eigenvalue of non-seasonal variations in SST from Weare *et al.* (1976).

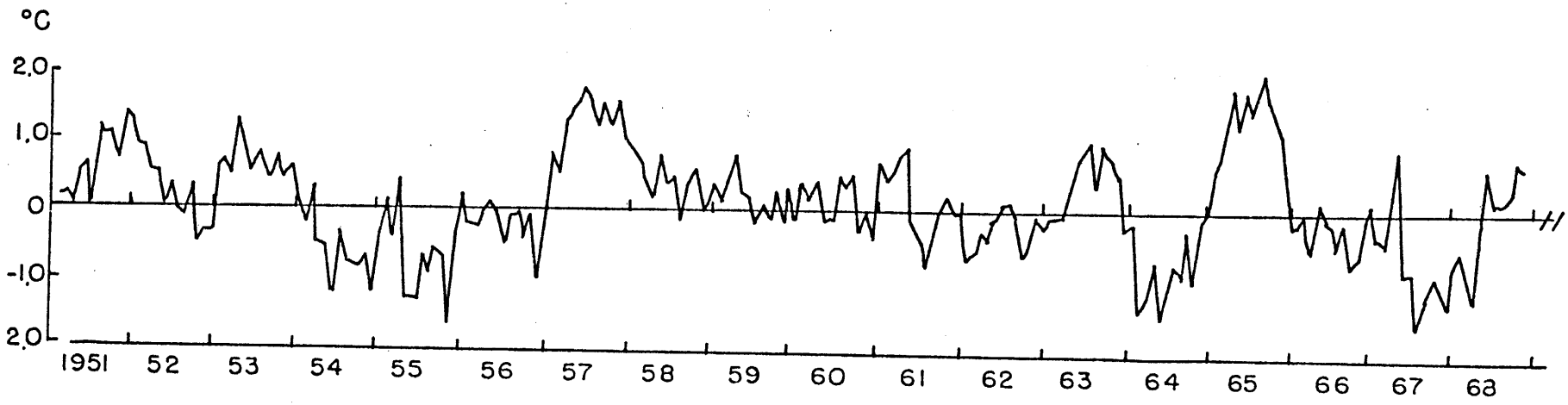

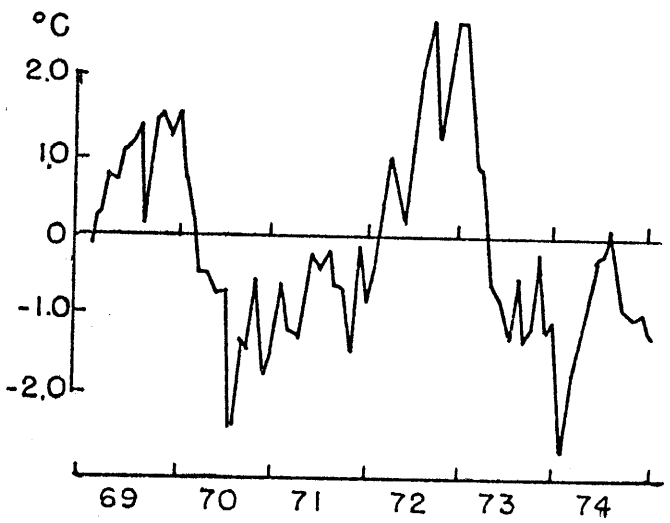

Figure 12. Time series of Zonal Mean Temperature (ZMT).

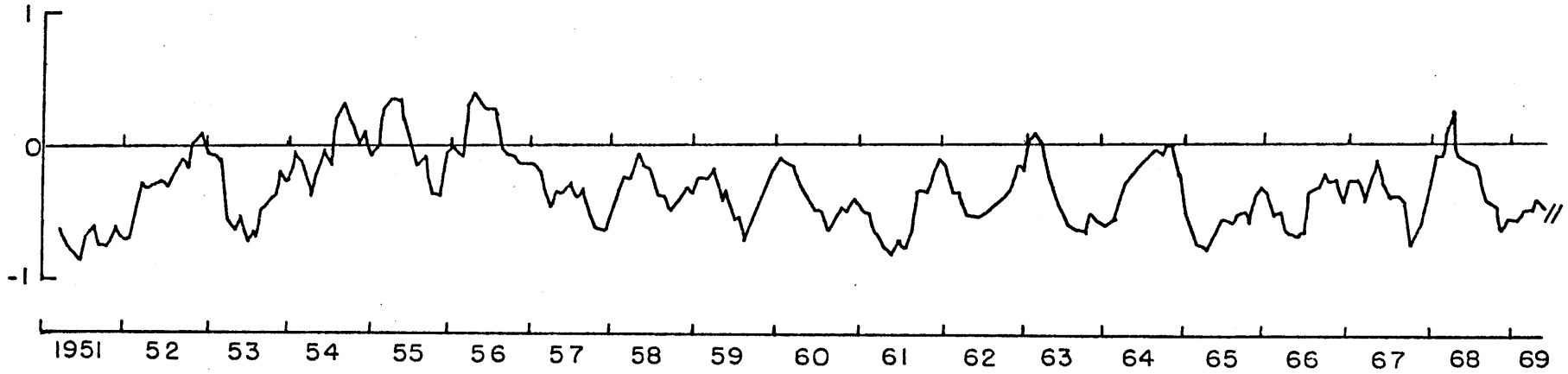

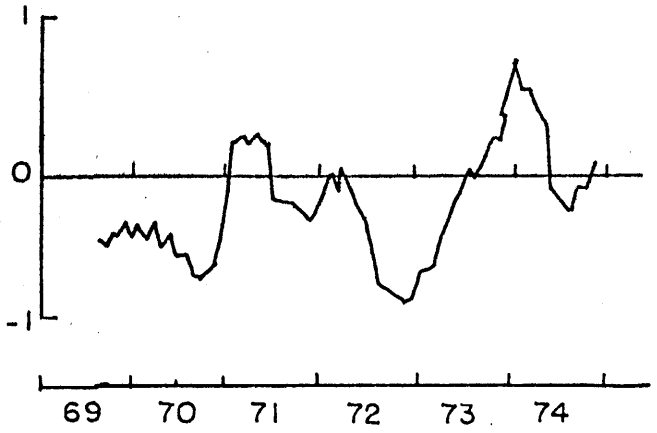

Figure 13. Austalian rainfall Index.

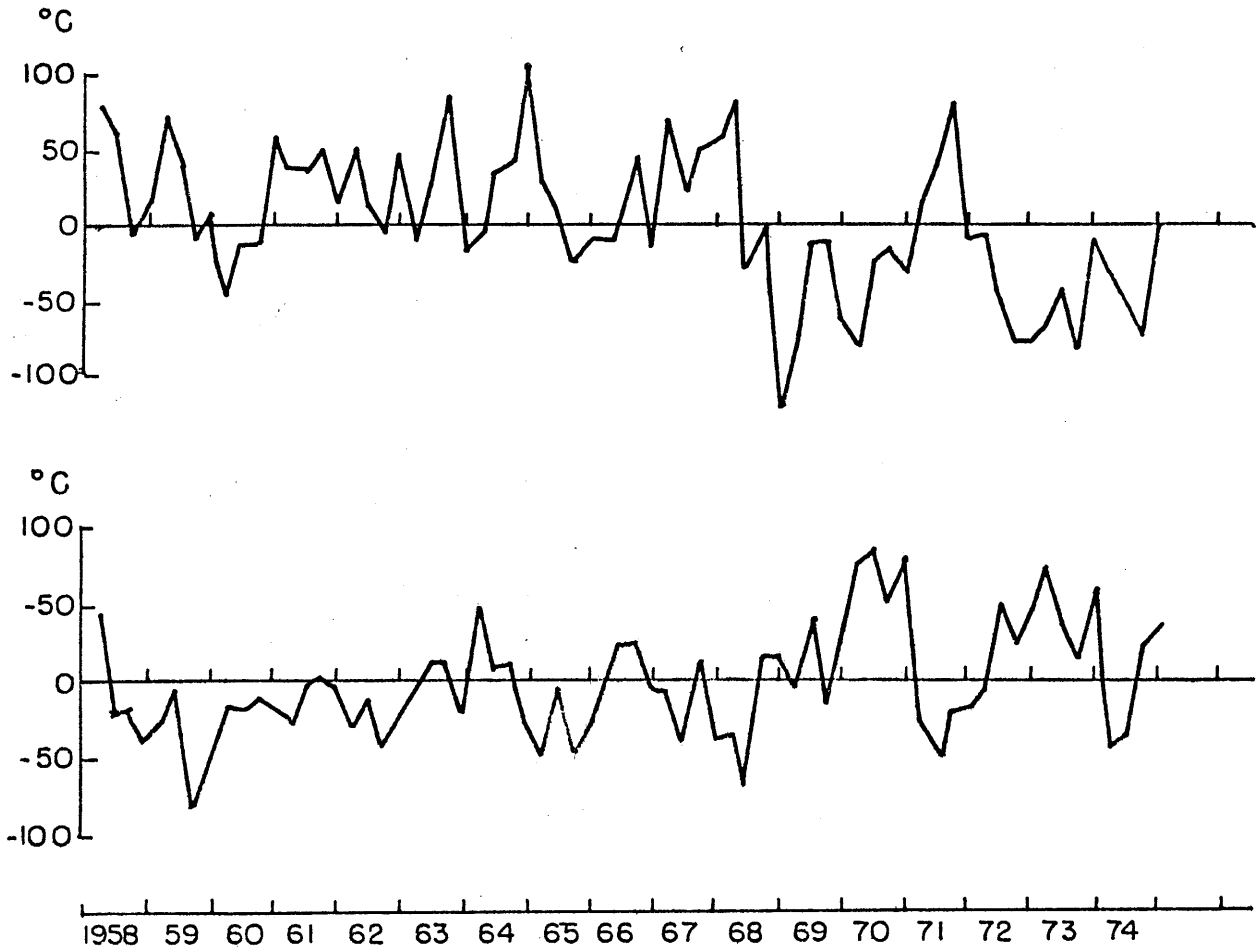

Figure 14. Meridional temperature gradients from Angell and Korshover (1978); (top) northern hemisphere; (bottom) southern hemisphere.

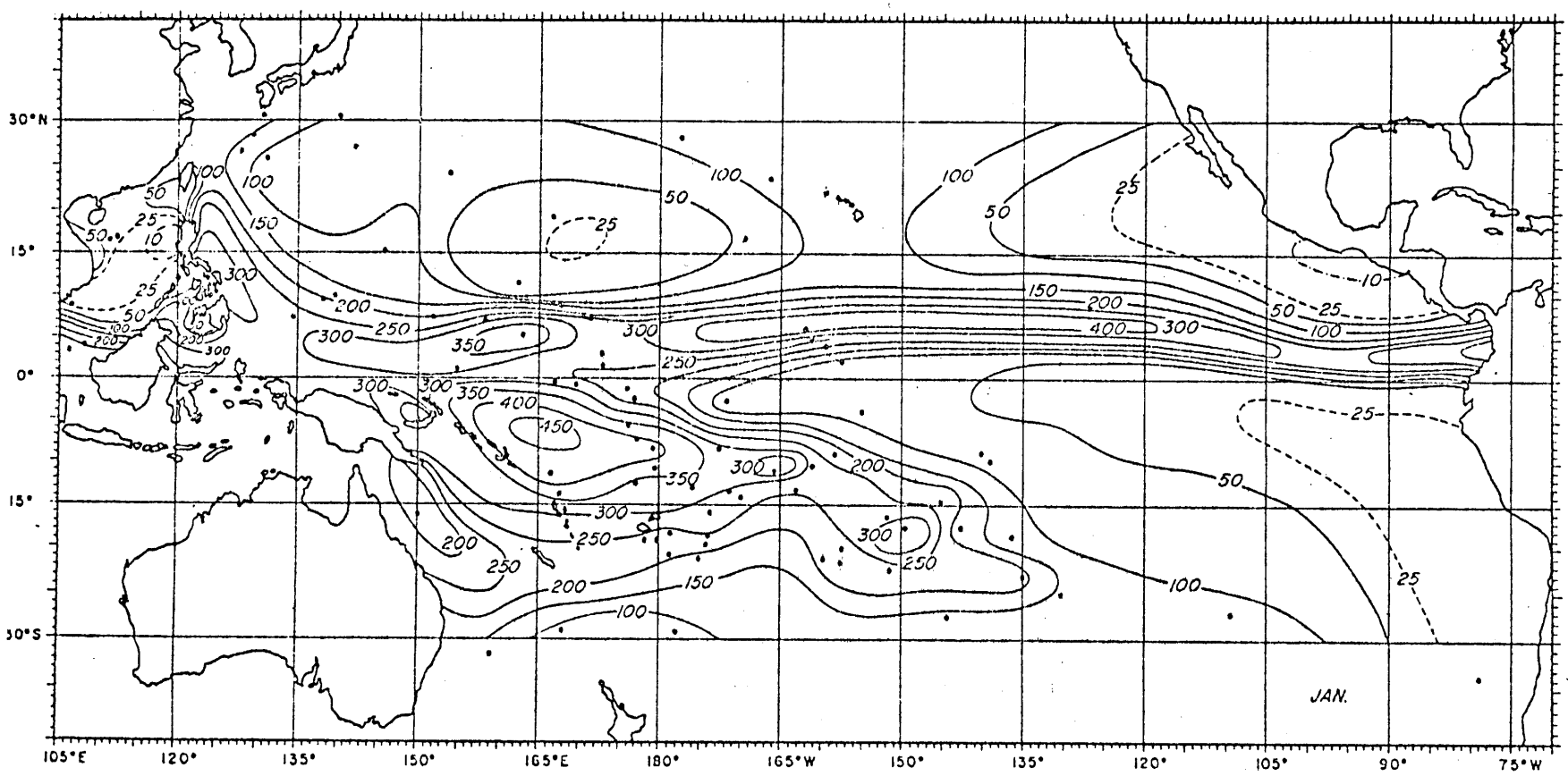

Figure 15. January precipitation from Taylor (1973), in millimeters.

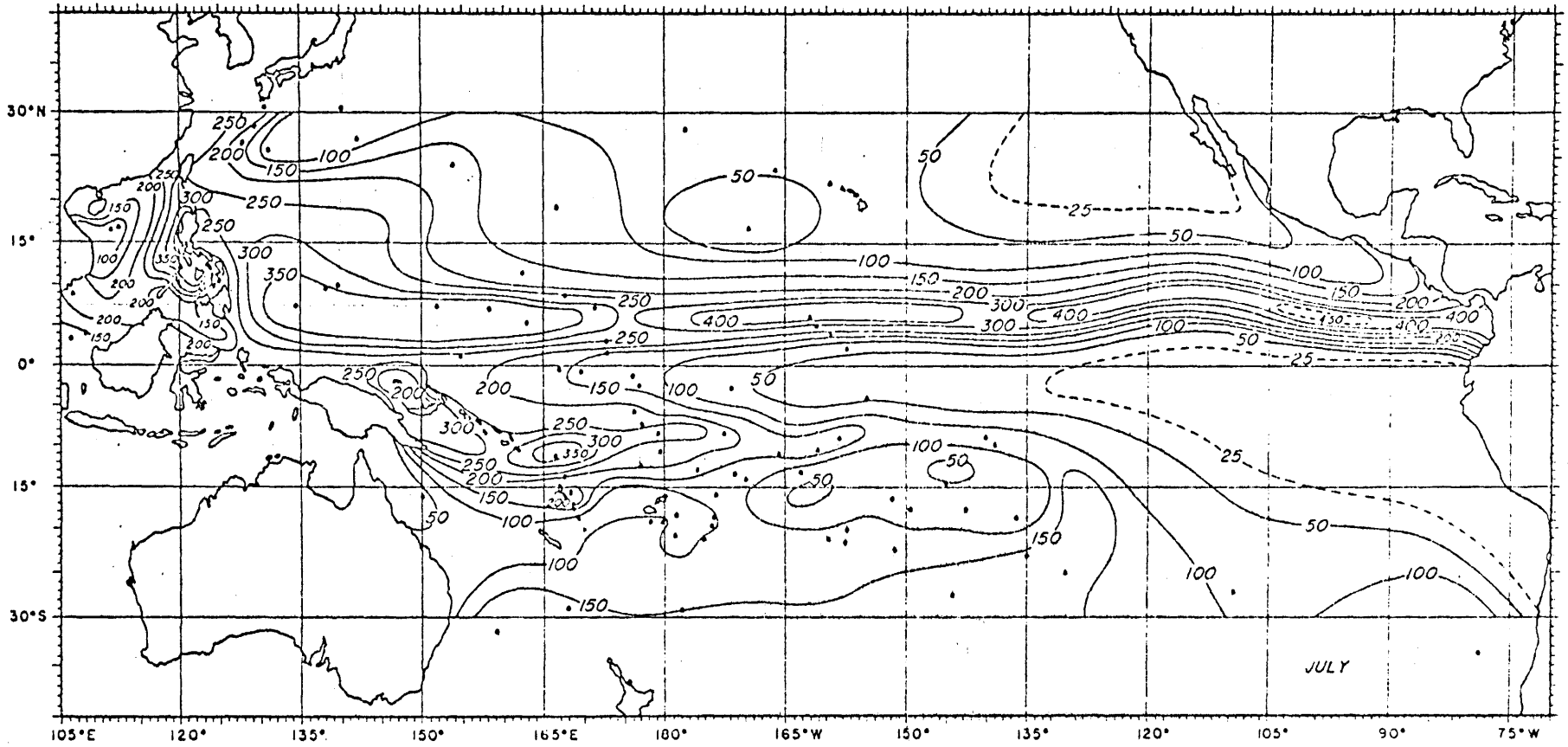

Figure 16. July precipitation from Taylor (1973), in millimeters.

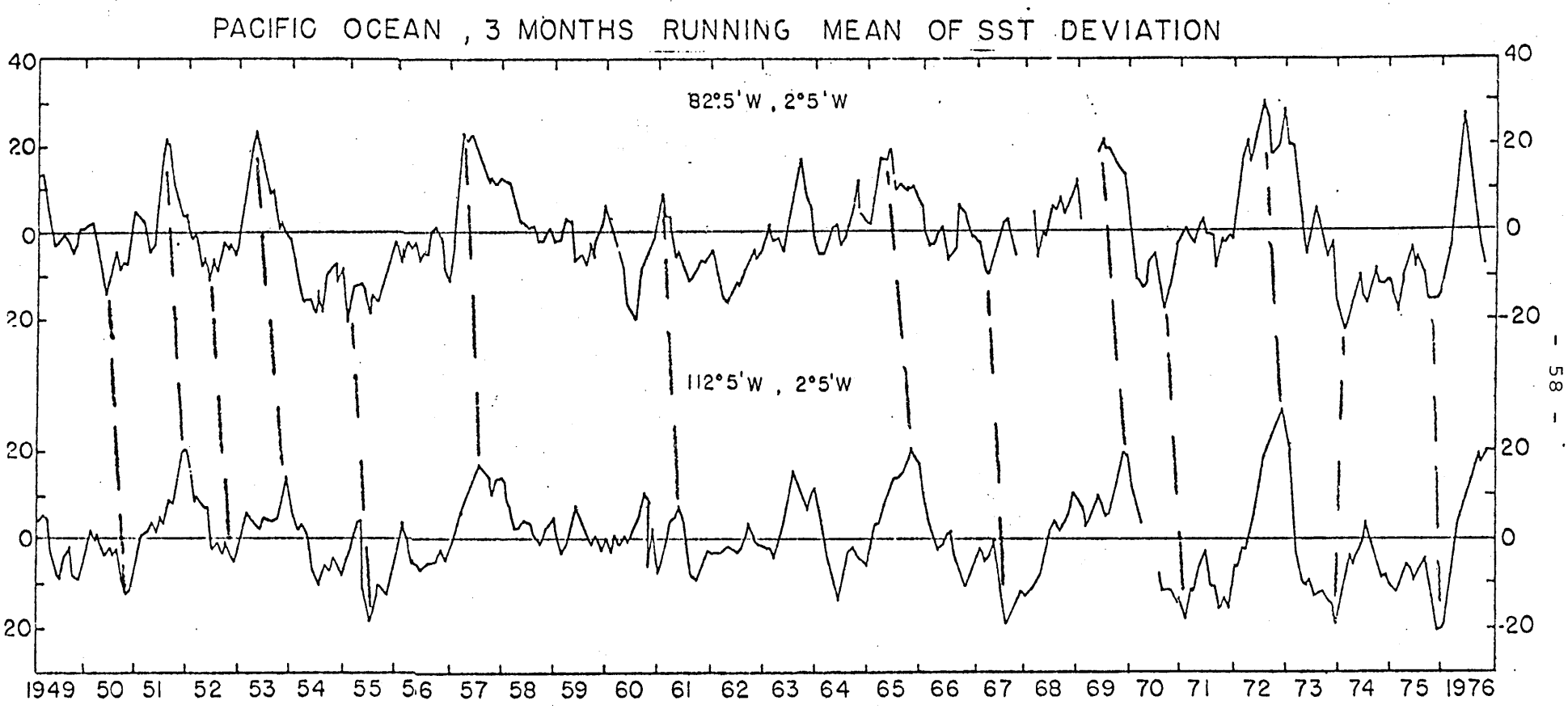

Figure 17. Time series of Pacific SST for indicated locations, from Newell (personal communication), in tenths of a degree Celsius.

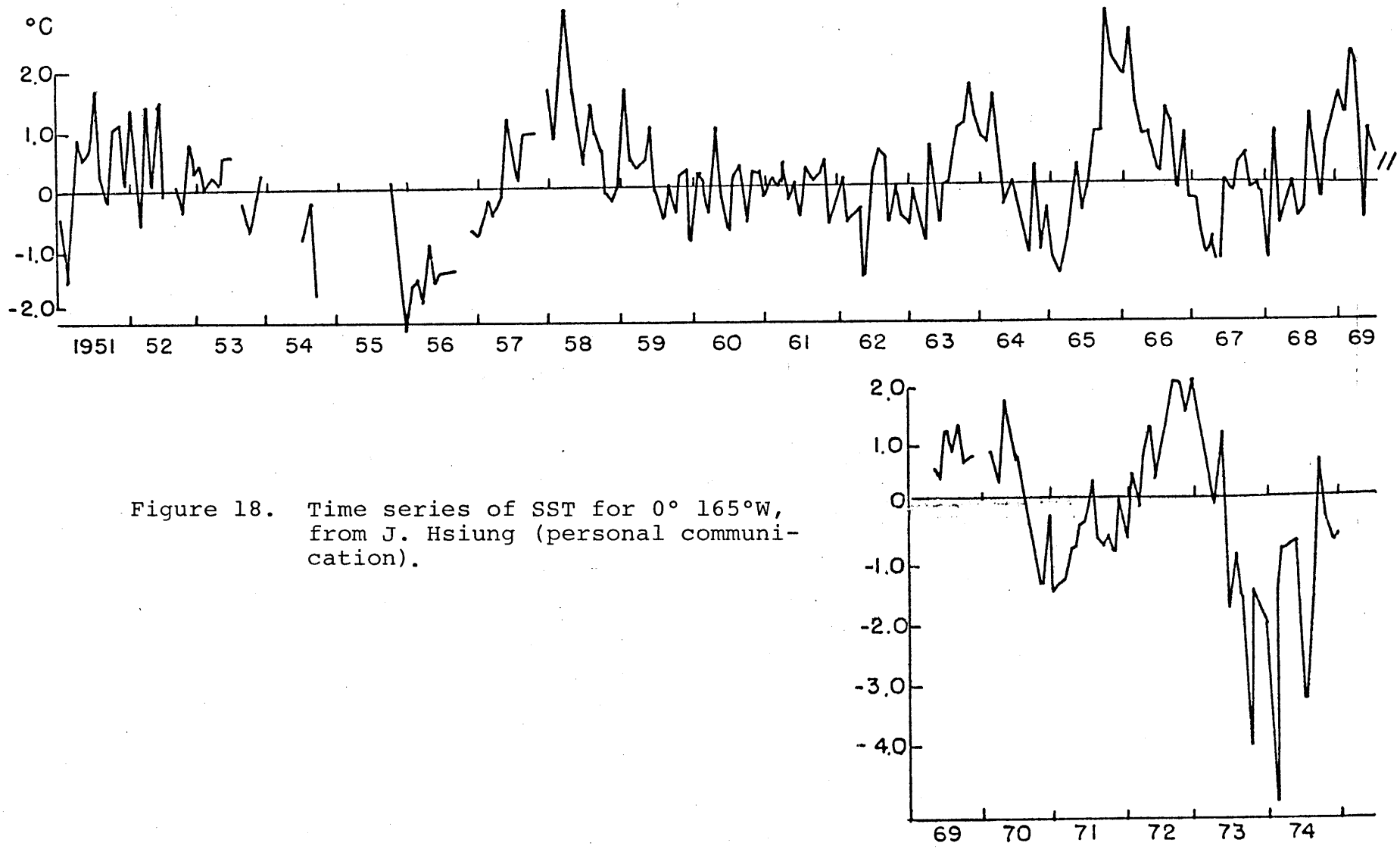

Figure 18. Time series of SST for 0° 165°W, from J. Hsiung (personal communication).

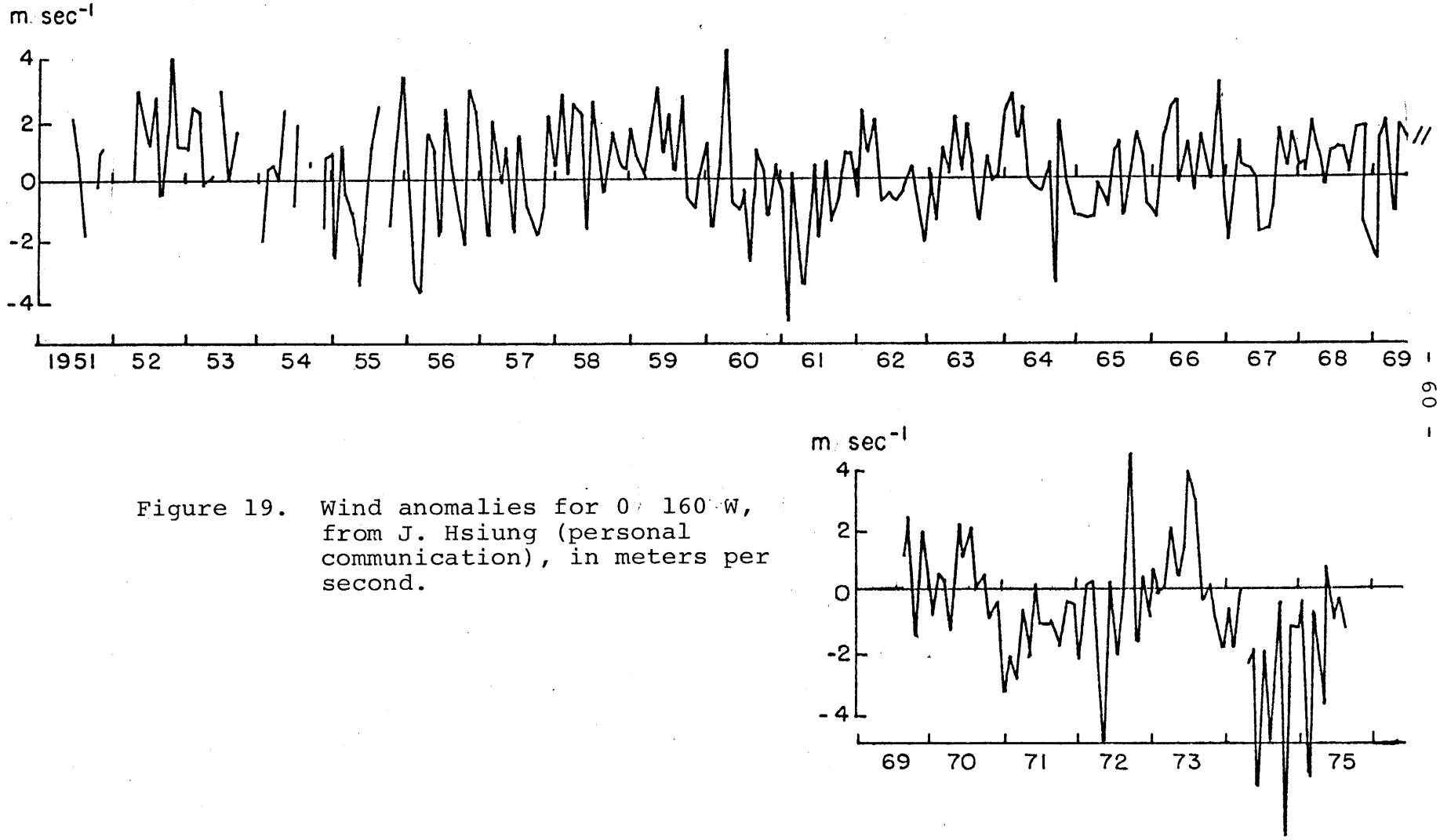

Figure 19. Wind anomalies for 0° 160° W, from J. Hsiung (personal communication), in meters per second.

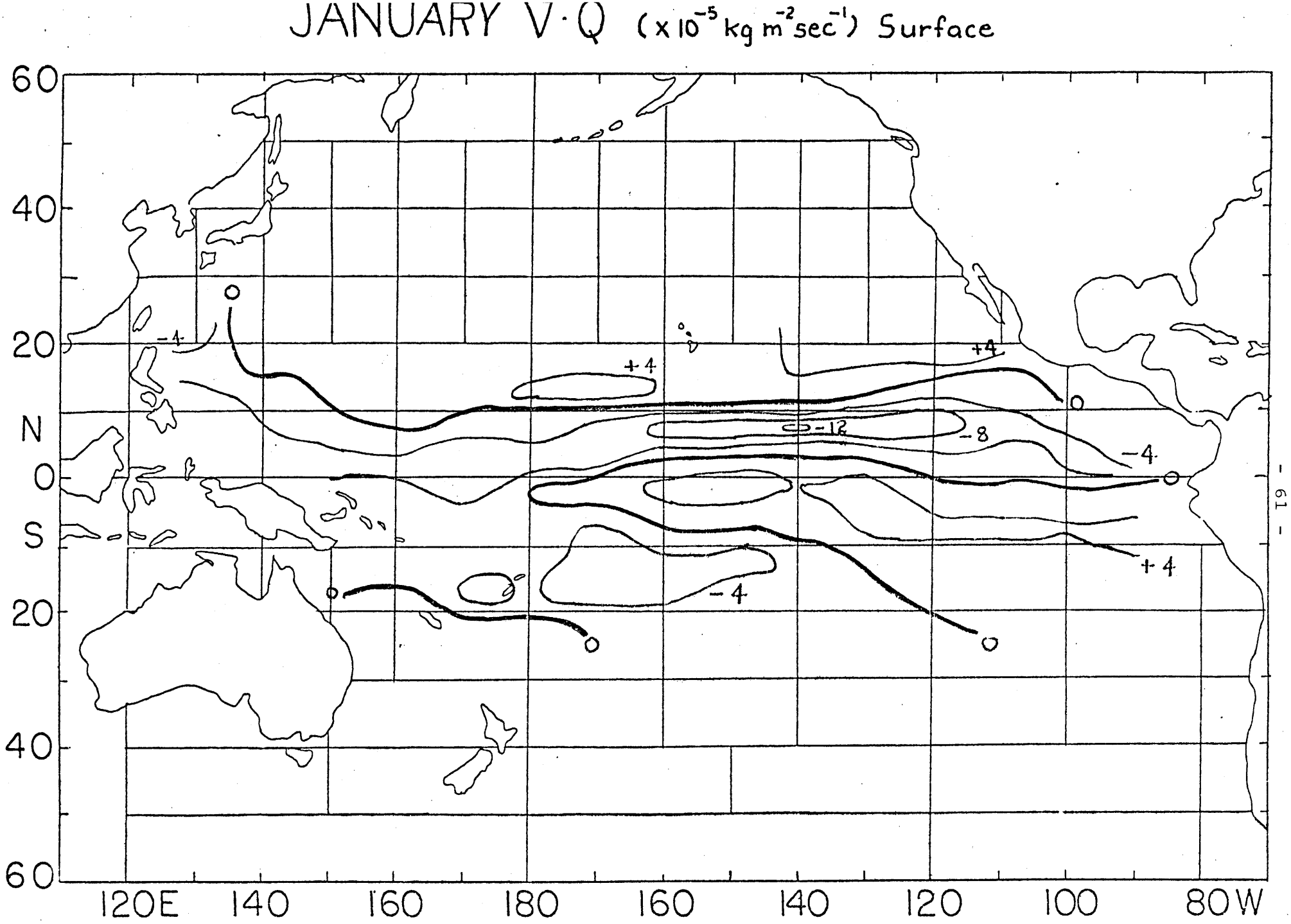

Figure 20. January moisture flux divergence

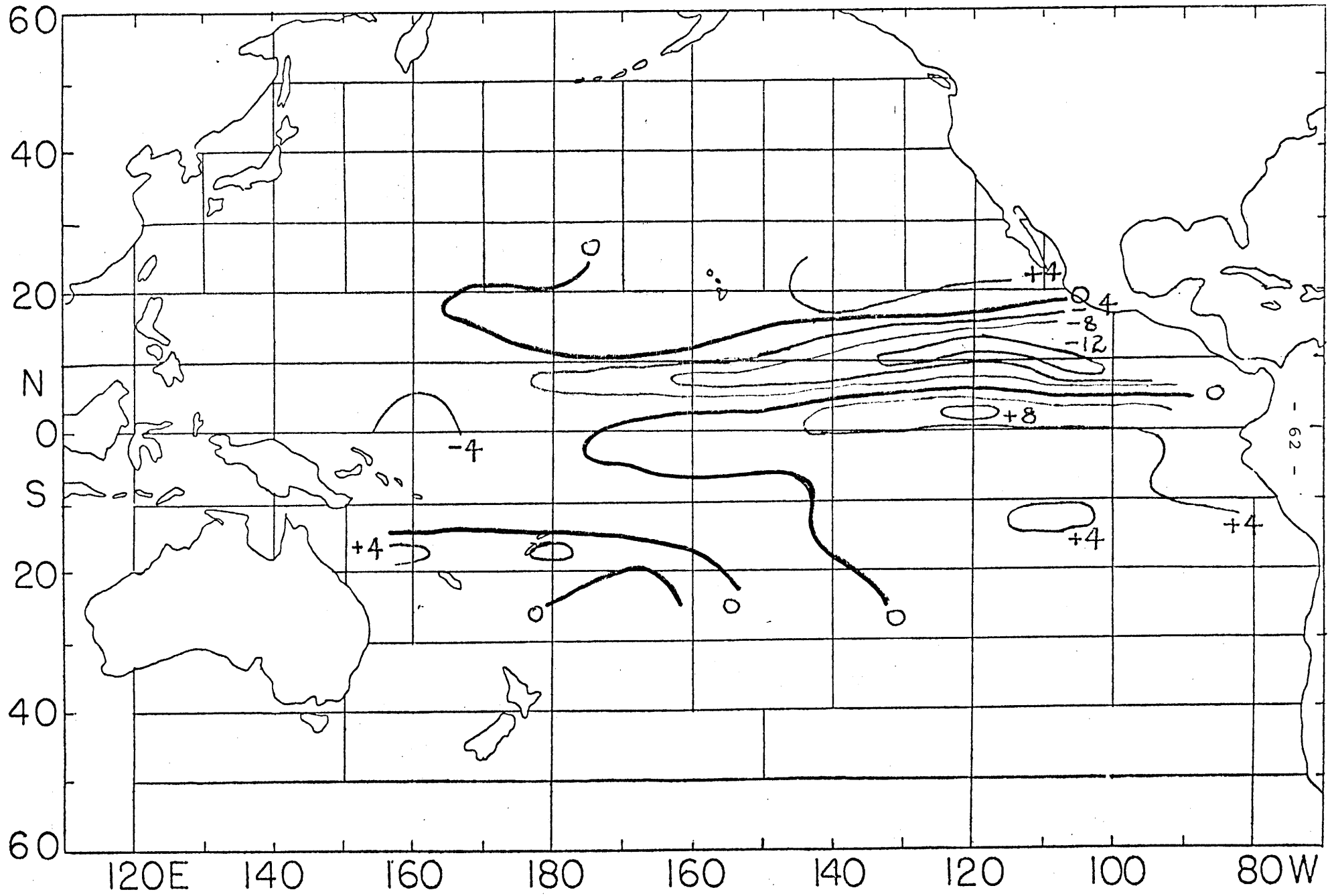

Figure 21. July moisture flux divergence

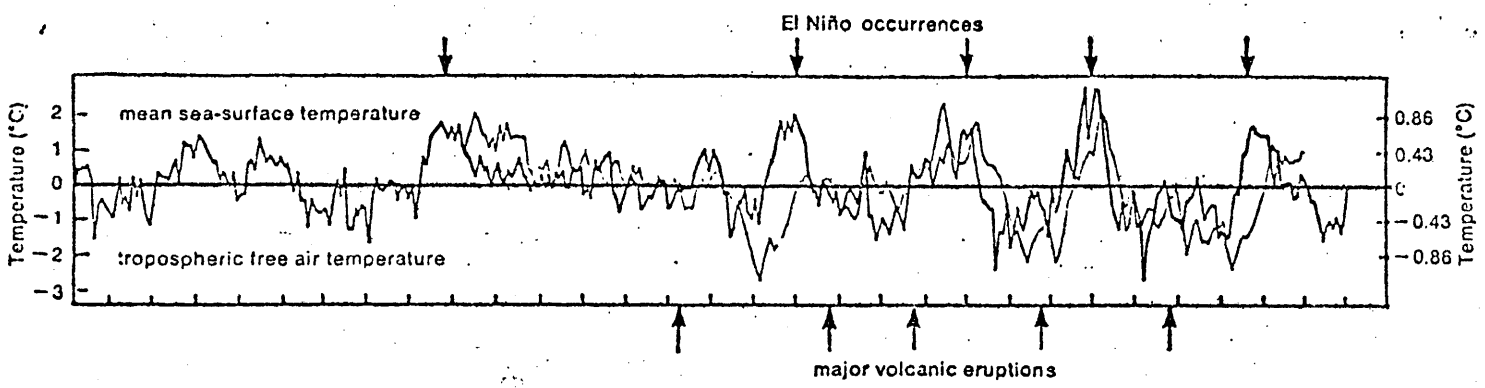

Figure 22. Temperature variations of SST and free air temperature from Newell (1979).

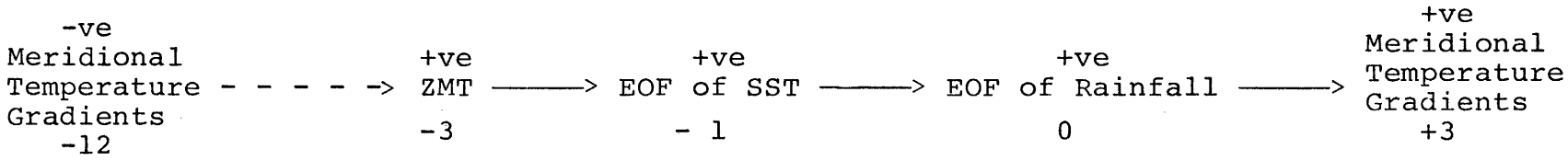

Figure 23. Chronological sequence of events from correlations

TABLE 1. Statistics of EOF calculation

	λ	Variance Explained (%)
1	1819.5	7.661
2	1189.0	5.007
3	1009.9	4.252
4	942.2	3.967
5	811.2	3.416

<——— Lag (Months) ———>											
-5	-4	-3	-2	-1	0	1	2	3	4	5	
0.336	0.419	0.524	0.614	0.690	0.742	0.761	0.751	0.735	0.664	0.603	EOF of SST
+0.208	+0.298	+0.406	+0.505	+0.586	+0.634	+0.659	+0.669	+0.677	+0.626	+0.580	ZMT
-0.087	0.041	0.169	0.269	0.320	0.245	0.124	-0.043	-0.211	-0.358	-0.304	N.H. Meridional* Temperature Gradient
-0.171	-0.014	0.203	+0.287	0.344	0.326	0.039	-0.134	-0.261	-0.338	-0.357	S.H. Meridional* Temperature Gradient
-0.140	+0.020	+0.208	+0.313	+0.374	+0.316	+0.099	-0.093	-0.263	-0.395	-0.370	Total Meridional* Temperature Gradient
-0.142	-0.196	-0.241	-0.310	-0.358	-0.400	-0.419	-0.409	-0.347	-0.315	-0.259	Australian Rainfall Index

TABLE 2. Correlations of the EOF of rainfall first eigenvalue time series with various quantities (positive lag means EOF lags quantity) (1951-1974).

(Note: Lags for starred quantities (*) are in seasons, not months.)

<——— Lag (Months) ———>											
-5	-4	-3	-2	-1	0	1	2	3	4	5	
-0.305	-0.312	-0.298	-0.312	-0.331	-0.335	-0.335	-0.285	-0.184	-0.101	-0.023	94120 Darwin
-0.203	-0.234	-0.246	-0.303	-0.328	-0.348	-0.355	-0.345	-0.271	-0.225	-0.172	94294 Townsville
-0.069	-0.093	-0.122	-0.203	-0.272	-0.339	-0.364	-0.374	-0.302	-0.260	-0.193	94367 Mackay
-0.076	-0.133	-0.188	-0.299	-0.354	-0.401	-0.404	-0.408	-0.357	-0.322	-0.272	94578 Brisbane

TABLE 3. Correlation of the EOF of rainfall first eigenvalue time series with normalized rainfall indices of various Australian stations, 1951-1974.

<——— Lag (Months) ———>										
-5	-4	-3	-2	-1	0	1	2	3	4	5
+0.052	+0.061	-0.010	-0.110	-0.293	-0.433	-0.438	-0.401	-0.244	-0.100	-0.054

TABLE 4. Correlation of the monsoonally stratified EOF of rainfall first eigenvalue with the monsoonally stratified Australian rainfall Index.